Climate warming and temporal variation in reproductive strategies in the endangered meadow viper

Jean-François Le Galliard, Malo Jaffré, Thomas Tully, Jean-Pierre Baron

Climate warming and temporal variation in reproductive strategies in the endangered meadow viper

Jean-François Le Galliard[1,2], Malo Jaffré[1], Thomas Tully[1], and Jean-Pierre Baron[1]

1. Sorbonne Université, CNRS, IRD, INRA, Institut d'écologie et des sciences de l'environnement (iEES Paris), 4 Place Jussieu, 75252 Paris Cedex 5, France

2. Ecole normale supérieure, PSL University, Département de biologie, CNRS, UMS 3194, Centre de recherche en écologie expérimentale et prédictive (CEREEP-Ecotron IleDeFrance), 11 chemin de Busseau, 77140 Saint-Pierre-lès-Nemours, France

Address correspondence to

Jean-François Le Galliard, CNRS, UMR 7618

Sorbonne Université, Institut d'écologie et des sciences de l'environnement (iEES Paris), 4 Place Jussieu, 75252 Paris Cedex 5, France

E-mail: galliard@biologie.ens.fr

Author contributions: JFLG, TT and JPB formulated the idea and designed the analyses, JPB collected the data with help from JFLG and TT, JFLG performed the analyses, MJ designed and analysed the model, JFLG wrote the manuscript and the other authors provided editorial advice.

Running headline: Climate warming and reproductive strategies in a viper

Summary

Anthropogenic climate change poses a significant threat to species on the brink of extinction. Many non-avian reptiles are endangered, but uncovering their vulnerability to climate warming is challenging because this requires analysing the climate sensitivity of different life stages and modelling population growth rates. Such efforts are currently hampered by a lack of long-term life history data. In this study, we used over three decades of mark-recapture data from a natural population of the endangered meadow viper (*Vipera ursinii ursinii*) to unravel the patterns of temporal variation in reproductive traits, the local climatic determinants of inter-annual variation in reproduction and the potential buffering effects of life cycle on population growth rate. We found significant inter-annual variation in body growth, gestation length, post-parturition body condition, clutch success and offspring traits at birth, while reproductive effort showed little temporal variation. Temperature during gestation was the most critical factor, reducing gestation length and increasing both clutch success and post-parturition body condition. In contrast, neither air humidity nor global radiation affected reproductive outcomes. This population had a negative growth rate with minimal temporal variation, indicating a rapid decline largely independent of climatic conditions. Overall, the viper's life history traits appeared to be buffered against temporal variation in climatic conditions, with this declining population potentially benefiting on the short-term from rising local temperatures.

Keywords: reproduction, body growth, temperature, rainfall, gestation.

Introduction

Habitat loss, overexploitation of wild populations for food or resources, and introduced alien species have pushed many species to the brink of extinction (Ceballos et al. 2020). Anthropogenic climate change is an aggravating extinction threat and thus plays a major role in the current biodiversity crisis (McLaughlin et al. 2002; Urban 2015). To improve our understanding of climate-driven extinction processes, a consensus has emerged on the need for integrated assessments of climate vulnerability (Williams et al. 2008; Huey et al. 2012). In this conceptual framework, extinction risk depends not only on exposure to climate change, but also on the sensitivity and resilience of the organism. Studying the extinction risk of species with complex life cycles, such as many iteroparous organisms or those living in highly seasonal environments, requires an understanding of the effects of climate change at different life stages, and the modelling of population growth rates (reviewed in Brodie et al. 2013).

In this context, long time series of demographic data from individually marked individuals are needed to decipher direct and delayed effects of climatic conditions, to account for potential compensatory responses across the life history, and to quantify specific effects of extreme weather events that rarely occur in nature (Williams et al. 2008; Brodie et al. 2013). Integrated climate vulnerability assessments exist for a few plants and animals, but are scarce for non-avian reptiles (turtles, lizards, snakes, and crocodiles) due to the paucity of long-term data sets for these organisms (Le Galliard et al. 2012; Böhm et al. 2013; Winter et al. 2016). Furthermore, non-avian reptiles are at high risk of extinction compared to other tetrapods, with more than 20% of existing species being currently threatened, but the specific threats posed by climate change remain highly uncertain for most of these organisms (Gibbons et al. 2000; Falaschi et al. 2019; Cox et al. 2022). Thus, long-term studies of reptile population dynamics are needed to improve our understanding of the patterns and processes of their declines (Diele-Viegas and Rocha 2018; Diele-Viegas et al. 2020).

Non-avian reptiles are highly sensitive to the direct effects of global warming due to their behavioural thermoregulatory strategies (i.e., ectothermy). Direct, negative effects of climate change may include increased mortality risks due to overheating (e.g., Kingsolver et al. 2013), sublethal effects due to reduced basking and foraging activities (e.g., Sinervo et al. 2010), disruption of energy balance (reviewed in Rutschmann et al. 2024), or increased likelihood of physiological dehydration (e.g., Kearney and Porter 2004). Such deleterious effects can alter early life stages, whose survival depends strongly on abiotic conditions, but also adult life stages, especially in viviparous species where females must optimally regulate their body temperature during a long gestation period (Shine 2003; Le Galliard et al. 2012). However, the cumulative effects of these stresses on population growth and viability are uncertain, as non-avian reptiles have also developed strategies to buffer the negative effects of climate variability (Le Galliard et al. 2012; Cox et al. 2022). For example, some are efficient thermoregulators and exploit habitat heterogeneity to maintain homeostasis, even under changing environmental conditions (Huey et al. 2012; Sunday et al. 2014). On the other hand, many iteroparous reptiles have low and flexible metabolic requirements and can cope with prolonged periods of starvation or chronic water deprivation (Shine 2005). Some are capital breeders, accumulating energy for several months or even years before breeding (Bonnet et al. 1998; Shine 2003). For these species, we expect small environmental fluctuations in cumulative lifetime reproductive success, even under changing climatic conditions. Unfortunately, studies quantifying the temporal variability of life history traits and population growth rates are rare in reptiles (but see Miller et al. 2011; Rodríguez-Caro et al. 2021; Warret Rodrigues et al. 2021).

Climate change may also have indirect effects on non-avian reptile populations via its impact on the quantity and distribution of food resources, or the abundance of predators (see Diele-Viegas and Rocha 2018 for a review). The trophic effects of climatic conditions have

been well studied in ecosystems characterized by resource pulses; for example, high rainfall regimes in certain arid or tropical environments favour greater prey abundance and thus have positive effects on the growth, reproduction, or survival of certain snake species (e.g., Ujvari et al. 2010; Meik et al. 2024). In temperate regions, climate change may also alter the prey community, with potentially variable effects on reptile demography between studies (Diele-Viegas and Rocha 2018). For example, in a viper population in Italy, whose phenology is highly dependent on ambient temperature, prey availability reflects local habitat variation rather than climatic conditions (Rugiero et al. 2012, 2013). In contrast, in another viper population in Sweden, an extreme summer climatic event caused a potential decline in resources that was associated with a loss of body condition and a reduction in future adult survival (Madsen et al. 2023). These trophic effects of climate change are likely to be more pronounced in reptiles with specialized diets and inflexible foraging behaviour (Ujvari et al. 2011; Diele-Viegas and Rocha 2018).

Among non-avian reptiles, vipers rank among the most endangered groups, with 16% of species threatened compared to 8% of all reptiles' species (Böhm et al. 2013; Maritz et al. 2016; Cox et al. 2022). Many snake populations are declining globally, primarily due to habitat loss or reduced prey availability (Reading et al. 2010; Luiselli et al. 2011; Böhm et al. 2013). However, changes in climatic conditions can also drive long-term population declines (e.g., Shine and Mason 2004; Pomara et al. 2014; Madsen et al. 2023). Snakes exhibit ecological traits that are sensitive to climate change, with higher temperatures generally enhancing activity levels, accelerating gestation, and improving the quality of reproduction in temperate species (Lourdais et al. 2004; Moreno-Rueda et al. 2009; Le Galliard et al. 2012; Rugiero et al. 2013). On the other hand, winter and summer climatic conditions can have variable effects on annual survival rates (Altwegg et al. 2005; Pomara et al. 2014; Elmberg et al. 2024). Extreme climate events, especially those leading to water shortage, are also likely to

disrupt resource availability and reproductive success (Dezetter et al. 2021; Holden et al. 2022; Madsen et al. 2023).

Here, we analysed over three decades of mark-recapture data from a population of the meadow viper (*Vipera ursinii ursinii*, Bonaparte 1835) to uncover patterns of temporal variation in reproductive traits, to identify the local climatic factors influencing these variations, and assess the potential buffering effects of life cycle on population growth rates. *Vipera u. ursinii* is a small viper with a fragmented distribution across medium-altitude mountain ranges in the northern Mediterranean basin. This species is listed on the IUCN Red List of threatened European species, although climate change is not currently identified as a primary threat (Ferchaud et al. 2011). Previous research on our study population has revealed that the meadow viper has a slow life history with a continuous growth throughout life, a sexual maturation at 3-5 years of age, a biennial breeding, and a high and stable annual subadult and adult survival (Baron et al., 1996, 2013; Tully et al., 2020). In our study population, the vipers primarily feed on large grasshoppers, which represents up to 99% of the diet during summer (Baron 1992). Although growth rates and some reproductive traits fluctuate from year to year, it is unclear whether this variability is linked to climatic conditions, or to what extent life history traits variability contribute to temporal variation in the population growth rate.

In this study, we quantified the effects of climatic variables related to the most relevant thermal and water constraints. Since the meadow viper is a capital breeder, alternating between breeding and non-breeding years (Baron et al. 2013; Tully et al. 2020), we tested for the effects of climatic condition during gestation, during the mating period prior to gestation, and during the preceding non-reproductive year. We next parametrized a finite stochastic integral projection model (Easterling et al. 2000; Vindenes et al. 2011; Jaffré and Le Galliard 2016) to (1) quantify the demographic and environmental variances in population growth rate,

and (2) identify the vital rates most critical for population growth. Our analysis revealed distinct patterns of climate-reproduction relationships, but minimal environmental variation in population growth rate. Our findings suggest limited potential for direct effects of climate warming on the vulnerability of this population.

Materials and methods

Study species and site

The meadow viper *V. u. ursinii* is a small insectivorous viper inhabiting open and dry calcareous grasslands between 900 and 2 200 m a.s.l. in the northern Mediterranean basin. This study was carried out in Mont Ventoux population (1430 m altitude, 44°18'N, 5°26'E), a population occupying an area of 100 ha that is isolated from the nearest populations 45 km away. A four hectares study area has been monitored continuously from 1979 until 2014, when monitoring was halted due to lack of support and conflicts with local landowners. The area is divided into two contiguous study sites of approximately two hectares each, including a north-facing and mesophilic hillside (habitat A), and a south-facing and xerophilic hillside (habitat B). Small home ranges averaging 0.09 ha (Baron et al. 1996), together with the presence of a 10 m wide asphalt road separating the two sites, make movements of snakes between these two sites extremely rare (only two such movements were reported during this study). In this population, females become sexually mature at approximately 4-6 years of age. Adult males and adult females emerge around mid-April and early May respectively. Vitellogenesis begins after hibernation and lasts 4 to 8 weeks. Mating occurs during the last two weeks of May, soon followed by ovulation and fertilization, which occurs during the first week of June. Parturition takes place between mid-August and mid-September, depending on weather conditions. Hibernation begins in October.

Demographic data collection

Snakes were individually marked by scale clipping upon their first capture during 56 primary capture sessions between 1979 and 2014 (n=1346 captures, mean duration per session of 10 days). Although scale clipping is highly reliable, we also recorded ventral and head scales to confirm the ventral scale clipping pattern. Primary capture sessions were carried out by 1-3 people for 1-2 weeks twice a year, including one session during the mating season and before ovulation, and one session before the end of gestation. All spotted animals were captured, identified and measured (snout-vent length, SVL to the nearest mm and body mass to the nearest dg). Sexual maturity and reproductive status (non-reproductive, reproductive: post-ovulation, gravid or post-partum) of each female was assessed. During the second capture session, ova were counted by palpation of the abdominal cavity to provide an accurate estimate of litter size (Baron et al. 2013). Snakes were released at their capture site in the evening of the day of capture, or after parturition for gravid females (see below). All applicable institutional and/or national guidelines for animal care and use were followed.

In 1983-1988 and from 1994 onwards, we obtained data on reproductive output by keeping gravid females in the laboratory until they gave birth (498 offspring, 162 litters, 109 mothers, 28 years). Gravid females were kept in individual rearing boxes (350 × 180 × 210 mm) with a shelter, damp soil, free access to water and a heat source to allow the snakes to thermoregulate. Body mass was measured daily. Immediately after parturition, the number of undeveloped ova, dead embryos, stillborns and healthy offspring were counted to calculate litter size and litter success (all variables are precisely defined in Baron et al. 2013). On average, females were kept in the laboratory for 15 days (± 10.7 SD, range = 0-46) prior to parturition, a short period of captivity that should not influence reproductive parameters. The gestation period was defined as the time between the date of ovulation (assumed to start on 10 June based on pers. obs.) and the date of parturition. Newborns were measured for SVL and

192 body mass, and sexed by counting sub-caudal scales. Mothers were released with their
193 offspring at the maternal capture site on average 11 days (± 7 SD) after parturition. Data on
194 survival and growth during the juvenile stage and data on intermittent reproduction and
195 longevity have been reported elsewhere (Baron et al. 2010a, 2013; Tully et al. 2020).

196 Climate data collection

197 Temperature and rainfall data were recorded since June 1992 by Météo France at a non-
198 automated weather station at the study site (Beaumont-Mont Serein, 1445 m a.s.l.,
199 44°10'48"N, 5°15'18"E). To reconstruct time series of weather data during the entire time
200 period of the census (1980-2014), we gathered temperature and rainfall data from an
201 automated meteorological station located 30 km south-west of the study site (Carpentras, 99
202 m a.s.l., 44°05'00"N, 5°03'30"E), and temperature, rainfall, global radiation and specific
203 humidity data calculated for the study site by the Safran model of Météo France (Quintana-
204 Seguí et al. 2008). The Carpentras station provides high quality and long term meteorological
205 data on temperature and precipitation, but is located at a lower altitude than the study site. The
206 Safran model is a gauge-based analytical meteorological system that provides reconstructed
207 and robust weather data through interpolation methods at 8 km resolution in France for the
208 period 1958-2014 (Vidal et al. 2010). We obtained daily data on precipitation (including
209 snowfall), minimum and maximum air temperature, specific humidity, wind speed and global
210 radiation for a grid cell centred on the study site. For this study, we calculated daily maximum
211 temperature (°C), daily cumulative rainfall (mm), daily cumulative global radiation (J/cm^2)
212 and daily mean of atmospheric specific humidity (g/kg) as climate variables (Appendix A).
213 We chose these variables because they are relevant to the thermal and water biology of
214 reptiles such as the meadow viper (Lourdais et al. 2004; Guillon et al. 2009; Le Galliard et al.
215 2012), and may correlate with environmental constraints on basking time (low daily
216 maximum temperatures and low global radiation) and environmental constraints on

evaporative water loss and water uptake (limited rainfall and low air specific humidity). For each climate variable and each study year, we calculated stage-specific weather data during the mating period (the three first weeks of May), the average gestation period (from the first week of June to the first week of September), and the non-reproductive period of the previous year (from the second week of June to the last week of September of the previous year). The non-reproductive period of the previous year was included to account for intermittent biennial reproduction and the capital breeding strategy of the species (Baron et al. 2013). In addition, we calculated the temperature conditions experienced during three consecutive gestation stages, namely early gestation (first week of June to first week of July), mid-gestation (first week of July to first week of August) and late gestation (first week of August to first week of September).

Statistical analyses

We first used mixed-effects models to investigate temporal variation (between years) and spatial variation (between sites A and B) in gestation length, total clutch size and clutch success (percentage of viable offspring in the clutch) controlling for body size, variation in clutch mass (including water and residual tissue from amnion and allantois) and variation in post-partum body condition (log-transformed body mass after parturition, controlling for log-transformed body size). We analysed clutch mass including post-partum body mass as a covariate, which amounts to examining variation in “relative clutch mas” (Van Dyke and Beaupre 2011). We also calculated mass change and body size growth of females during their non-reproductive years (57 observations, 35 females), as we have previously shown that females stop growing and lose significant body mass during the reproductive years (Baron et al. 2013). Models for for body mass change and body size growth included initial body mass and initial body size as covariates in the models, respectively, to account for the slowing of growth with age (Baron et al. 2010b). Inter-individual differences were also tested prior to full

model implementation, but we found that these were negligible compared to inter-annual differences so we did not include them in our final models. We also analysed spatial and temporal variation in offspring characteristics, including mass and body condition at birth. Body condition at birth was defined as the residual of a linear regression of body mass against SVL. Body mass was preferred to SVL for analyses of variation in offspring size because (1) offspring mass can be measured more accurately than SVL, (2) mass better reflects maternal energy allocation to the offspring than SVL, and (3) mass at birth is often used in studies of temporal variation in offspring fitness traits in reptiles (Baron et al. 2010a).

In all cases, we followed the methodology of Pinheiro and Bates (2000) for general linear models (normally distributed data) and of Bolker et al. (2009) for generalized linear models (binomially distributed data). In all models, habitat (site A vs. B) was included as a fixed effect and year was included as a random effect. We used a random intercept model, which assumes that years vary in the mean values of each response trait. We also checked for temporal autocorrelation by calculating the empirical autocorrelation function for the within-group residuals of the fitted models and found that temporal autocorrelation was negligible. For offspring traits, we included the random effect of litter identity, nested within birth year and habitat effects. Mixed models were fitted using the *lme* package (Pinheiro et al. 2022) in R 3.2.4 software (R Core Team 2020). Model assumptions (normality, homoscedasticity and/or overdispersion) were checked and met in all cases.

We first used these models to quantify variation between years and maternal identity, controlling for fixed effects of critical covariates (body size and habitat). Fixed effects were tested with conditional F-tests based on REML and random effects were tested with likelihood ratio tests. Initial models included all factors and model selection was performed backwards by removing non-significant terms until a minimum adequate model was obtained (all factors $p > 0.05$ removed). From the minimum adequate model, we calculated the ratio of annual

variation to the sum of annual and residual variation, hereafter referred to as relative temporal variation (RTV).

In a second step, we used the minimum adequate model as a starting point to search for the most influential weather covariates at each life stage. Following our investigation of all climate variables (see below), we tested for effects of temperature, global radiation and specific humidity calculated during the mating, gestation and non-reproductive periods on reproductive traits with a significant inter-annual variation (see below). We compared all models with additive effects of each covariate and therefore did not test for interactions or quadratic effects. We however checked graphically for the absence of quadratic effects of climatic conditions (results not shown). We compared the independent effects of temperature, global radiation and specific humidity to determine which weather variable was the best predictor of inter-annual variation. Where climatic conditions during gestation were retained in the best model, we next tested more specifically for the effects climatic conditions calculated during early (first month), mid (second month) or late (third month) gestation period. Models were compared by Akaike Information Criterion corrected for small sample size (AICc), Akaike's weight (*wi*) and evidence ratio (ER) using the *MuMIn* (Multiple-Model Inference) package (MuMIn, Bartoń 2022). In addition, we calculated the marginal pseudo-R2 (R2m) and the conditional pseudo-R2 (R2c) for each mixed-effects model using the *r.squaredGLMM* function of the *MuMin* package (Nakagawa and Schielzeth 2013). The best set of models included all models within a cumulative Akaike's weight < 0.95, and the best models were considered to be those with an AICc difference with the best model < 2 (Burnham and Anderson 1998, see Appendix B for a list of model selection tables). Relative variable importance was calculated as the sum of *wi* of all models including the variable, and parameter estimates were estimated using a model averaging procedure (conditional average). Results are presented as mean ± SE unless otherwise stated.

Results

Climate variation

Supplementary information on temporal variation and correlation patterns between climate variables are provided in Appendix A. The weather at the study site showed marked seasonal variation, with harsh thermal conditions for reptile activity from November to April (daily maximum temperatures around and below 5°C and daily minimum temperatures below 0°C), a short summer season from June to August (daily maximum temperatures above 15°C and daily minimum temperatures above 10°C), and heavy rainfall or snowfall from September to May (cumulative monthly rainfall or snowfall greater than 100 mm). The temperature and rainfall data collected at the study site since 1992 were highly correlated with those of the Safran model available on a long-term basis, allowing time series of temperature and rainfall conditions to be reconstructed for the entire duration of the population survey. There was a weak pattern of increasing daily maximum temperatures in late spring and early summer over time during the study, but not for average summer temperatures (see Appendix A and Figure A1). Global radiation increased significantly over time during the survey (Figure A1). Cumulative rainfall and air specific humidity showed no temporal trend. Independent of these trends, weather data showed strong inter-annual variation at all reproductive stages. As rainfall at the study site was less well predicted by the Safran data, and was also negatively correlated with global radiation and positively correlated with air specific humidity, we did not use rainfall data in our statistical models of life history variation in vipers.

Life history variation

Similar to previous findings (Baron et al. 2013; Tully et al. 2020), certain reproductive traits and body growth were significantly influenced by maternal body size and habitat (Table 1). Larger females produced larger litters, exhibited higher clutch success, and gave birth to

larger offspring. Additionally, females from the xerophilic habitat (Habitat B) displayed similar size-independent fecundity and reproductive effort to those of females from the mesophilic habitat (Habitat A). However, they exhibited lower post-parturition body condition, reduced offspring condition, and smaller body size growth and annual change than females from Habitat A. Moreover, we detected significant inter-annual variation in all demographic traits, except for total clutch size (Table 1). RTV was generally low for reproductive effort , where it was largely driven by a few years with unusually low reproductive effort and also for offspring mass. Intermediate levels were observed for clutch success, post-parturition body condition, offspring condition and body size growth. The highest RTV was recorded for gestation length and annual changes in body mass during non-reproductive years (detailed results provided in Table 1).

Climate effects on reproduction and growth

Our model selection procedure included 17 candidate models and one null model (the minimum adequate models shown in Table 1, see Appendix B for the full list of all models). We excluded from the set of candidate models some models with additive effects of global radiation variables due to strong collinearity between the variables (see Appendix A). The combined outcomes from our model selection procedures for gestation length (Table B1), clutch success (Table B2), relative clutch mass (Table B3), post-parturition body condition (Table B4) and offspring mass and condition (Tables B5 and B6) showed very small effects of specific humidity, moderate effects of global radiation and significant positive effects of air temperature.

The gestation length shortened significantly with increasing average temperatures during both the mating period (-1.46 days/°C ± 0.48, z = 2.92, P = 0.003) and gestation (-2.76 days/°C ± 0.96, z = 2.73, P = 0.006; Figure 1, Table B1), with relative importance (*w*) of 0.94 and 0.93 respectively. It also tended to shorten with hotter thermal conditions during the

previous non-reproductive season (w = 0.46). The best model, which included average temperature during gestation (Table B1, wi = 0.49), outperformed the three other gestation-stage dependent models. The second-best model included effects of temperature during early gestation (wi = 0.45). Upon re-analysing the data excluding the coldest summer season, which saw a high number of clutch failures (Figure 1A), we obtained similar results, with even stronger effects of temperatures (gestation: -3.75 days/°C ± 0.79, z = 4.5, P < 0.0001; mating: -1.57 days/°C ± 0.38, z = 3.92, P < 0.0001).

Climatic conditions explained little variation in relative clutch mass, with all covariates showing relative importance below 0.25 (Table B2). The most influential covariate was global radiation during the previous summer season, and it negatively affected relative clutch mass (-0.009 ± 0.004, z = 1.97, P = 0.05, result not shown). In sharp contrast, thermal conditions were major drivers of inter-annual variation in post-parturition body condition (Table B3). Average temperature during gestation was the most influential variable (w = 0.66), followed by average temperature during the previous year (positive effect, w = 0.48) and during the mating period (negative effect, w = 0.45). Post-parturition body condition increased with rising average temperatures during gestation (0.031 ± 0.014 g/°C, z = 2.1, P = 0.04; Figure 2A). Based on additional analyses, we found that late gestation thermal conditions were the primary driver of this pattern (wi = 0.65; 0.024 ± 0.009 g/°C, z = 2.4, P = 0.01).

Clutch success increased on average with higher mean temperature during gestation (logit regression: 0.45 ± 0.21, z = 2.1, P = 0.04; Figure 2B, Table B4, w = 0.51), and was moderately influenced by temperature and humidity during the previous non-reproductive season (w = 0.34 and w = 0.21, respectively). Additional analyses indicated that the model with average temperature during gestation fitted equally well the data than a model with average temperature during mid-gestation (wi = 0.49 and wi = 0.45, respectively). Climatic conditions did not significantly influence offspring mass at birth (Table B5, all w < 0.22).

However, both mean global radiation (w = 0.54, 0.0006 ± 0.0002, z = 2.9, P = 0.004) and temperature during gestation (w = 0.24, 0.05 ± 0.02, z = 2.1, P = 0.04) were positively correlated with offspring condition at birth. Lastly, annual changes in body mass and body growth during the non-reproductive years were unaffected by climatic conditions during the active summer season (all w < 0.23, not shown).

Population growth analysis

We fitted a finite stochastic integral projection model (IPM) to the meadow viper life cycle and analysed the stochastic IPM using the methodology described in Jaffré and Le Galliard (2016, see Appendix C). The deterministic IPM predicted a substantial annual population decline of approximately 12% ( ), consistent with previous findings using a matrix population model (Baron et al. 1996). Components of stochastic growth included a significant demographic variance ( ) and a very weak environmental variance ( ), indicating that the iteroparous life cycle with a constant adult survival and breeding frequency buffered the population against temporal variation in growth, juvenile survival and reproduction. In addition, an analysis of the elasticity of the deterministic growth rate to changes in the kernel function of the IPM revealed (1) very low sensitivity to changes in adult reproduction, (2) strong sensitivity to the survival and growth of juveniles and immature females, and (3) moderate sensitivity to the survival and growth of older sexually mature individuals (Figure 3A). Using a realistic starting population size of 100 vipers, the stochastic model predicted a median extinction time of 25–30 years for this population, with complete extirpation of the population likely within less than a century (Figure 3B). Given the weak contribution of reproduction to growth rate, climate warming effects on reproductive traits is unlikely to significantly alter this extinction trajectory.

Discussion

Our analysis complements previous research on body growth rate strategies, survival, intermittent reproduction, and ageing in the same meadow viper population (Baron et al. 2010a, b, 2013; Tully et al. 2020). In particular, our findings reveal that fecundity and reproductive effort are largely buffered against environmental variation and are primarily dictated by female body size. Female fecundity is strongly constrained by body size and exhibit little to no variability among years. Similarly, reproductive effort, defined as the relative mass lost during gestation (Bonnet et al. 2002; Van Dyke and Beaupre 2011), shows minimal inter-annual variation, except for one year marked by a notably poor reproduction without any clear climatic explanation (Table 1). These results contrast with the pronounced year-to-year variation in reproductive effort and frequency seen in other snake species, which often occurs in response to changes in food availability. For example, some snakes feed on prey whose populations fluctuate dramatically due to changes in rainfall patterns, leading to pronounced reproductive variability in those species (Madsen and Shine 1999; Lourdais et al. 2002; Ujvari et al. 2010). This discrepancy likely stems from the meadow viper's unique semi-insectivorous diet, which consists almost exclusively of crickets and grasshoppers. At our study site, these insects are both diversified and abundant during the summer activity season (Baron 1992), indicating that food resources are unlikely to be limiting factors and this stable supply of food may contribute to the low variability in reproductive traits observed in this population.

In contrast to fecundity and reproductive effort, we observed a strong temporal variability in annual growth rates during non-reproductive years, as well as in traits related to gestation speed, body condition, and reproduction quality. These variations were either unrelated to climatic conditions even during extreme climate years, such as body growth of adult females and body mass of young at birth, or were linearly correlated with ambient

414 temperature rather than air humidity (which indicates desiccation risk due to evaporative
415 water loss) or global radiation (which indicates both thermoregulatory conditions and
416 rainfall). In general, warmer ambient conditions are more favourable for reproduction by
417 accelerating gestation, improving post-parturition condition, and ensuring better offspring
418 condition at birth.

419 The flexibility of gestation length and post-partum body condition, which is driven by
420 warmer temperatures, is not surprising but demonstrates that reproductive traits can be
421 flexible without significantly affecting reproductive effort or frequency. This should be
422 understood in the light of the meadow viper's bioenergetic strategy of biennial reproduction
423 and resource capitalization (Bonnet et al. 1998; Baron et al. 2013; Huang et al. 2013). Females
424 alternate between breeding years – marked by a halt in structural growth and depletion of
425 body reserves – and non-breeding years, during which growth resumes and body condition is
426 restored to a threshold necessary for future reproduction (Baron et al. 2013). Our findings
427 suggest that warmer ambient temperatures during gestation accelerate reserve capitalization
428 dynamics but do not alter the biennial threshold for reproduction (Madsen and Shine 1999;
429 Baron et al. 2013; Huang et al. 2013; Capula et al. 2016). These effects on reserve dynamics
430 are unlikely to influence future survival, as survival is not linked to post-partum body
431 condition (Baron et al. 2013).

432 In contrast, lowland populations of the asp viper (*Vipera aspis*) exhibit a more
433 semelparous reproductive strategy, where higher gestation temperatures result in poorer body
434 condition by the end of gestation (Lourdais et al. 2002, 2004). One explanation for this
435 difference is that meadow vipers are able to feed during gestation, unlike carnivorous vipers
436 that are anorexic due to the challenge of consuming large preys while gravid (Bonnet et al.
437 2002; Baron et al. 2013). Thus, we hypothesize that warmer thermal conditions during
438 gestation may favour maternal feeding in meadow vipers, enabling them to recoup the energy

439 expenditure of viviparity more efficiently. Our analysis further suggests that thermal
440 conditions toward the end of gestation, during late summer, are particularly important for
441 maintaining female energy balance and reserve dynamics.

442 The impact of ambient temperatures on the speed of gestation reflects a general effect of
443 thermal conditions on the rate of biological processes in ectotherms, even including years of
444 heat waves that might have slowed gestation by altering daily activities during the hottest
445 times of the day. Such phenological changes are common in many temperate non-avian
446 reptiles (Lourdais et al. 2004; Moreno-Rueda et al. 2009; Rugiero et al. 2013; Diele-Viegas
447 and Rocha 2018). Here, it corresponded to a shift of about three weeks between the coldest
448 and warmest years, a pattern very similar to that observed in the asp viper (Lourdais et al.
449 2004; Lorioux et al. 2013). In this congeneric species, thermal conditions during mid-
450 gestation are more strongly correlated with gestation length, whereas our study suggests that it
451 is the average temperature over the entire gestation that is most important. Thus, generally
452 warmer summer conditions, in early, mid or late gestation, will accelerate gestation similarly.
453 The demographic consequences of shifts in reproductive phenology are likely to be small in
454 meadow vipers, as the date of parturition does not affect the future maternal or neonate
455 survival, growth and sexual maturation (Baron et al. 2010a, 2013).

456 A notable demographic effect of climatic conditions is a positive correlation between
457 average temperatures during gestation and reproductive success, measured by the proportion
458 of viable neonates in the litter. This trend holds even when accounting for data from the
459 extreme heat wave of 2003, when summer temperatures were unusually high and could have
460 imposed sublethal stress on reproduction. Overall, reproductive success is typically high in
461 this species, but cooler years are associated with an increased frequency of developmental
462 failures and prolonged, incomplete gestations. This reflects the importance of optimal
463 thermoregulation during gestation for embryo development and viability in vipers (Lorioux et

al. 2013). Altogether, we found that some reproductive traits in this population are currently constrained by cold thermal conditions. Thus, assuming other factors remain constant, climate warming is likely to provide short-term benefits to this population, a pattern that may apply more generally to high-altitude reptiles, whose energy budgets are constrained by colder and shorter activity seasons (Huang et al. 2013). Comparative data and mechanistic models could be used to determine whether this trend is consistent across the species' range. For example, similar studies could examine populations in southern regions or at lower elevations, which are closer to the species' upper thermal limits, to see if they respond differently to climate warming.

We integrated the effects of the different vital rates and their temporal variability on long-run growth rate and population dynamics using the Integral Projection Model framework (Easterling et al. 2000; Ellner and Rees 2006; Vindenes et al. 2011). The motivation for building this model is the existence of a high variability in body size, with pervasive effects of individual size on growth, sexual maturation, fecundity, or the size of newborns at birth. Our analysis of an individual-based version of the model allows for both demographic fluctuations generated by random, identically and independently distributed temporal variability in each vital rate (i.e., environmental stochasticity) and random inter-individual variability in the demographic processes of growth, survival, and reproduction (i.e., demographic stochasticity). This shows that temporal fluctuations in the stochastic growth rate are negligible compared to random inter-individual demographic fluctuations in the meadow viper. Assuming that the average stochastic growth rate scales like  (Vindenes et al. 2011; Jaffré and Le Galliard 2016), the population size at which the contribution of demographic variance equals contribution of environmental variance would be approximately 1,000 females in this population, well above the estimated population size of a few hundred vipers (Baron et al. 1996). This result is expected for long-lived species with low temporal

variability in adult survival and an iteroparous reproductive mode that spreads fecundity over several years (Hilde et al. 2020). As a result, stochastic population dynamics are dominated first by a significant deterministic decay term that predicts rapid decline, and second by a strong demographic stochasticity term that accelerates this deterministic decline in small populations. Instead, climate variability is unlikely to slow down or accelerate average stochastic growth. These predictions confirm previous estimates from matrix population models and are consistent with the population decline observed at this isolated site (Ferrière et al. 1996). Climate warming could still benefit the population by improving clutch success, a vital rate positively related to population growth. Yet, average clutch success is already high (around 80%) and our analysis shows that the population growth rate is not as sensitive to components of the life cycle related to reproduction as it is to those related to growth and survival.

Our study has implications for assessing the conservation status of the meadow viper and designing measures to protect at least the Mont Ventoux population in France. We show that temporal variability and climatic conditions currently have a limited demographic impact on this population, with warmer temperatures even providing beneficial for breeding. Thus, climate change should not be considered an immediate threat to this population. However, continued monitoring is essential to track the potential effects of more extreme weather conditions, such as summer intense and prolonged hot and dry periods (Madsen et al. 2023). Future assessments should also consider indirect threats posed by climate warming, such as the upward migration of lowland species that could outcompete or prey on meadow vipers, as well as long-term changes in vegetation and habitat. Meanwhile, our analysis underlines the urgent need for strong conservation measures to prevent the expected rapid population of the Mont Ventoux meadow viper. The population's deterministic growth is low, and reversing the decline will require joint improvements of several critical life history traits such as growth and

survival. Previous research found that growth and late-life survival are enhanced in more humid microhabitats (Tully et al. 2020), suggesting that effective conservation actions could include habitat restoration. Strict protection measures to decrease disturbance and mortality could also be adopted. These could include physical barriers, clear signage, and active surveillance to safeguard the population.

Acknowledgements

We are grateful to DIREN PACA and MEEDDAT for providing capture permits (08/004/DEROG) during our fieldwork and to the many workers who helped to collect data in the field.

Declarations

Funding. This research has been partly supported by the Centre National de la Recherche Scientifique and by the Agence Nationale de la Recherche program 07-JCJC-0120. **Conflicts of interest.** Not applicable. **Ethics approval.** Ethics approval was not required for this study according to local legislation. **Consent to participate.** Not applicable. **Consent for publication.** Not applicable. **Availability of data and code.** The data and codes were deposited in Zenodo under the reference number DOI: 10.5281/zenodo.10219671.

Supporting Information

Supporting Information is available for this article online: Appendix A. Climate variability; Appendix B. Model selection tables; Appendix C. Integral projection model

533 # Literature cited

Altwegg R, Dummermuth S, Anholt BR, Flatt T (2005) Winter weather affects asp viper *Vipera aspis* population dynamics through susceptible juveniles. Oikos 110:55–66. https://doi.org/10.1111/j.0030-1299.2001.13723.x

Baron J-P (1992) Régime et cycles alimentaires de la vipère d'Orsini (*Vipera ursinii* Bonaparte 1835) au Mont Ventoux, France. Rev Ecol Terre Vie 47:287–311. https://doi.org/10.3406/revec.1992.2408

Baron J-P, Ferrière R, Clobert J, Saint Girons H (1996) Stratégie démographique de *Vipera ursinii* au Mont-Ventoux. Comptes Rendus Académie Sci Paris 319:57–69

Baron J-P, Le Galliard J-F, Tully T, Ferrière R (2013) Intermittent breeding and the dynamics of ressource allocation to growth, reproduction and survival. Funct Ecol 27:173–183. https://doi.org/10.1111/1365-2435.12023

Baron J-P, Le Galliard J-F, Tully T, Ferrière R (2010a) Cohort variation in offspring growth and survival: prenatal and postnatal factors in a late-maturing viviparous snake. J Anim Ecol 79:640–649. https://doi.org/10.1111/j.1365-2656.2010.01661.x

Baron J-P, Tully T, Le Galliard J-F (2010b) Sex-specific fitness returns are too weak to select for non random patterns of sex allocation in a viviparous snake. Oecologia 164:369–378. https://doi.org/10.1007/s00442-010-1660-y

Bartoń K (2022) MuMIn: Multi-Model Inference

Böhm M, Collen B, Baillie JEM, et al (2013) The conservation status of the world's reptiles. Biol Conserv 157:372–385. https://doi.org/10.1016/j.biocon.2012.07.015

Bolker BM, Brooks ME, Clark CJ, et al (2009) Generalized linear mixed models: a practical guide for ecology and evolution. Trends Ecol Evol 24:127–135. https://doi.org/10.1016/j.tree.2008.10.008

Bonnet X, Bradshaw D, Shine R (1998) Capital versus income breeding: an ectothermic perspective. Oikos 83:333–342. https://doi.org/10.2307/3546846

Bonnet X, Lourdais O, Shine R, Naulleau G (2002) Reproduction in a typical capital breeder: costs, currencies and complications in the aspic viper. Ecology 83:2124–2135. https://doi.org/10.1890/0012-9658(2002)083[2124:RIATCB]2.0.CO;2

Brodie JF, Post ES, Doak DF (2013) Wildlife Conservation in a Changing Climate. University of Chicago Press

Burnham KP, Anderson DR (1998) Model selection and inference: a practical information-theoretical approach. Springer Verlag, New York

Capula M, Rugiero L, Capizzi D, et al (2016) Long-term, climate-change-related shifts in feeding frequencies of a Mediterranean snake population. Ecol Res 31:49–55. https://doi.org/10.1007/s11284-015-1312-0

Ceballos G, Ehrlich PR, Raven PH (2020) Vertebrates on the brink as indicators of biological annihilation and the sixth mass extinction. Proc Natl Acad Sci 117:13596–13602. https://doi.org/10.1073/pnas.1922686117

Cox N, Young BE, Bowles P, et al (2022) A global reptile assessment highlights shared conservation needs of tetrapods. Nature 605:285–290. https://doi.org/10.1038/s41586-022-04664-7

Dezetter M, Le Galliard JF, Guiller G, et al (2021) Water deprivation compromises maternal physiology and reproductive success in a cold and wet adapted snake *Vipera berus*. Conserv Physiol 9:. https://doi.org/10.1093/conphys/coab071

Diele-Viegas LM, Figueroa RT, Vilela B, Rocha CFD (2020) Are reptiles toast? A worldwide evaluation of Lepidosauria vulnerability to climate change. Clim Change 159:581–599. https://doi.org/10.1007/s10584-020-02687-5

Diele-Viegas LM, Rocha CFD (2018) Unraveling the influences of climate change in Lepidosauria (Reptilia). J Therm Biol 78:401–414. https://doi.org/10.1016/j.jtherbio.2018.11.005

Easterling MR, Ellner SP, Dixon PM (2000) Size-specific sensitivity: applying a new structured population model. Ecology 81:694–708. https://doi.org/10.1890/0012-9658(2000)081[0694:SSSAAN]2.0.CO;2

Ellner SP, Rees M (2006) Integral projection models for species with complex demography. Am Nat 167:410–428. https://doi.org/10.1086/499438

Elmberg J, Palmheden L, Edelstam C, et al (2024) Climate change-induced shifts in survival and size of the worlds' northernmost oviparous snake: A 68-year study. PLOS ONE 19:e0300363. https://doi.org/10.1371/journal.pone.0300363

Falaschi M, Manenti R, Thuiller W, Ficetola GF (2019) Continental-scale determinants of population trends in European amphibians and reptiles. Glob Change Biol 25:3504–3515. https://doi.org/10.1111/gcb.14739

Ferchaud AL, Lyet A, Cheylan M, et al (2011) High genetic differentiation among French populations of the Orsini's viper (*Vipera ursinii ursinii*) based on mitochondrial and microsatellite data: implications for conservation management. J Hered 102:67–78. https://doi.org/10.1093/jhered/esq098

Ferrière R, Sarrazin F, Legendre S, Baron J-P (1996) Matrix population models applied to viability analysis and conservation: theory and practice with ULM software. Acta Oecologica 17:629–656

Gibbons JW, Scott DE, Ryan TJ, et al (2000) The global decline of reptiles, Deja Vu amphibians. Bioscience 50:653–666. https://doi.org/10.1641/0006-3568(2000)050[0653:TGDORD]2.0.CO;2

Guillon M, Guiller G, DeNardo DF, Lourdais O (2009) Microclimate preferences correlate with contrasted evaporative water loss in parapatric vipers at their contact zone. Can J Zool 92:81–86. https://doi.org/10.1139/cjz-2013-0189

Hilde CH, Gamelon M, Sæther B-E, et al (2020) The Demographic Buffering Hypothesis: Evidence and Challenges. Trends Ecol Evol 35:523–538. https://doi.org/10.1016/j.tree.2020.02.004

Holden KG, Gangloff EJ, Miller DAW, et al (2022) Over a decade of field physiology reveals life-history specific strategies to drought in garter snakes (*Thamnophis legans*). Proc R Soc B Biol Sci 289:20212187. https://doi.org/10.1098/rspb.2021.2187

Huang S-P, Chiou C-R, Lin T-E, et al (2013) Future advantages in energetics, activity time, and habitats predicted in a high-altitude pit viper with climate warming. Funct Ecol 27:446–458. https://doi.org/10.1111/1365-2435.12040

Huey RB, Kearney MR, Krockenberger A, et al (2012) Predicting organismal vulnerability to climate warming: roles of behaviour, physiology and adaptation. Philos Trans R Soc B Biol Sci 367:1665–1679. https://doi.org/10.1098/rstb.2012.0005

Jaffré M, Le Galliard J-F (2016) Population viability analysis of plant and animal populations with stochastic integral projection models. Oecologia 182:1031–1043. https://doi.org/10.1007/s00442-016-3704-4

Kearney M, Porter WP (2004) Mapping the fundamental niche: Physiology, climate, and the distribution of a nocturnal lizard. Ecology 85:3119–3131. https://doi.org/10.1890/03-0820

Kingsolver JG, Diamond SE, Buckley LB (2013) Heat stress and the fitness consequences of climate change for terrestrial ectotherms. Funct Ecol 27:1415–1423. https://doi.org/10.1111/1365-2435.12145

Le Galliard J-F, Massot M, Baron J-P, Clobert J (2012) Ecological effects of climate change on European reptiles. In: Brodie JF, Post E, Doak D (eds) Wildlife conservation in a changing climate. University of Chicago Press

Lorioux S, Vaugoyeau M, DeNardo DF, et al (2013) Stage Dependence of Phenotypical and Phenological Maternal Effects: Insight into Squamate Reptile Reproductive Strategies. Am Nat 182:223–233. https://doi.org/10.1086/670809

Lourdais O, Bonnet X, Guillon M, Naulleau G (2004) Climate affects embryonic development in a viviparous snake, *Vipera aspis*. Oikos 104:551–560. https://doi.org/10.1111/j.0030-1299.2004.12961.x

Lourdais O, Bonnet X, Shine R, et al (2002) Capital-breeding and reproductive effort in a variable environment: a longitudinal study of a viviparous snake. J Anim Ecol 71:470–479. https://doi.org/10.1046/j.1365-2656.2002.00612.x

Luiselli L, Madsen T, Capizzi D, et al (2011) Long-term population dynamics in a Mediterranean aquatic snake. Ecol Res 26:745–753. https://doi.org/10.1007/s11284-011-0828-1

Madsen T, Loman J, Bauwens D, et al (2023) The impact of an extreme climatic event on adder (*Vipera berus*) demography in southern Sweden. Biol J Linn Soc 138:282–288. https://doi.org/10.1093/biolinnean/blac147

Madsen T, Shine R (1999) The adjustment of reproductive threshold to prey abundance in a capital breeder. J Anim Ecol 68:571–580. https://doi.org/10.1046/j.1365-2656.1999.00306.x

Maritz B, Penner J, Martins M, et al (2016) Identifying global priorities for the conservation of vipers. Biol Conserv 204:94–102. https://doi.org/10.1016/j.biocon.2016.05.004

McLaughlin JF, Hellmann JJ, Boggs CL, Ehrlich PR (2002) Climate change hastens population extinctions. Proc Natl Acad Sci 99:6070–6074. https://doi.org/10.1073/pnas.052131199

Meik JM, Watson JA, Schield DR, et al (2024) Climatic temperature and precipitation jointly influence body size in species of western rattlesnakes. R Soc Open Sci 11:240345. https://doi.org/10.1098/rsos.240345

Miller DA, Clark WR, Arnold SJ, Bronikowski AM (2011) Stochastic population dynamics in populations of western terrestrial garter snakes with divergent life histories. Ecology 92:1658–1671. https://doi.org/10.1890/10-1438.1

Moreno-Rueda G, Pleguezuelos JM, Alaminos E (2009) Climate warming and activity period extension in the Mediterranean snake *Malpolon monspessulanus*. Clim Change 92:235–242. https://doi.org/10.1007/s10584-008-9469-y

Nakagawa S, Schielzeth H (2013) A general and simple method for obtaining R2 from generalized linear mixed-effects models. Methods Ecol Evol 4:133–142. https://doi.org/10.1111/j.2041-210x.2012.00261.x

Pinheiro JC, Bates D, R Core Team (2022) nlme: Linear and Nonlinear Mixed Effects Models

Pinheiro JC, Bates DM (2000) Mixed-effect models in S and S-plus. Springer, New York

Pomara LY, LeDee OE, Martin KJ, Zuckerberg B (2014) Demographic consequences of climate change and land cover help explain a history of extirpations and range contraction in a declining snake species. Glob Change Biol 20:2087–2099. https://doi.org/10.1111/gcb.12510

Quintana-Seguí P, Le Moigne P, Durand Y, et al (2008) Analysis of near-Surface atmospheric variables: validation of the SAFRAN analysis over France. J Appl Meteorol Climatol 47:92–107. https://doi.org/10.1175/2007JAMC1636.1

R Core Team (2020) R: A Language and Environment for Statistical Computing

Reading CJ, Luiselli LM, Akani GC, et al (2010) Are snake populations in widespread decline? Biol Lett 6:777–780. https://doi.org/10.1098/rsbl.2010.0373

Rodríguez-Caro RC, Capdevila P, Graciá E, et al (2021) The limits of demographic buffering in coping with environmental variation. Oikos 130:1346–1358. https://doi.org/10.1111/oik.08343

Rugiero L, Milana G, Capula M, et al (2012) Long term variations in small mammal composition of a snake diet do not mirror climate change trends. Acta Oecologica 43:158–164. https://doi.org/10.1016/j.actao.2012.07.002

Rugiero L, Milana G, Petrozzi F, et al (2013) Climate-change-related shifts in annual phenology of a temperate snake during the last 20 years. Acta Oecologica 51:42–48. https://doi.org/10.1016/j.actao.2013.05.005

Rutschmann A, Perry C, Le Galliard J-F, et al (2024) Ecological responses of squamate reptiles to nocturnal warming. Biol Rev 99:598–621. https://doi.org/10.1111/brv.13037

Shine R (2003) Reproductive strategies in snakes. Proc R Soc Lond B 270:995–1004. https://doi.org/10.1098/rspb.2002.2307

Shine R (2005) Life-history evolution in reptiles. Annu Rev Ecol Syst 36:23–46. https://doi.org/10.1146/annurev.ecolsys.36.102003.152631

Shine R, Mason RT (2004) Patterns of mortality in a cold-climate population of garter snakes (*Thamnophis sirtalis parietalis*). Biol Conserv 120:201–210. https://doi.org/10.1016/j.biocon.2004.02.014

Sinervo B, Mendez-de-la-Cruz F, Miles DB, et al (2010) Erosion of lizard diversity by climate change and altered thermal niches. Science 328:894–899. https://doi.org/10.1126/science.1184695

Sunday JM, Bates AE, Kearney MR, et al (2014) Thermal-safety margins and the necessity of thermoregulatory behavior across latitude and elevation. Proc Natl Acad Sci 111:5610–5615. https://doi.org/10.1073/pnas.1316145111

Tully T, Galliard J-FL, Baron J-P (2020) Micro-geographic shift between negligible and actuarial senescence in a wild snake. J Anim Ecol 89:2704–2716. https://doi.org/10.1111/1365-2656.13317

Ujvari B, Andersson S, Brown G, et al (2010) Climate-driven impacts of prey abundance on the population structure of a tropical aquatic predator. Oikos 119:188–196. https://doi.org/10.1111/j.1600-0706.2009.17795.x

Ujvari B, Shine R, Madsen T (2011) How well do predators adjust to climate-mediated shifts in prey distribution? A study on Australian water pythons. Ecology 92:777–783. https://doi.org/10.1890/10-1471.1

Urban MC (2015) Accelerating extinction risk from climate change. Science 348:571–573. https://doi.org/10.1126/science.aaa4984

Van Dyke JU, Beaupre SJ (2011) Bioenergetic components of reproductive effort in viviparous snakes: costs of vitellogenesis exceed costs of pregnancy. Comp Biochem Physiol -Mol Integr Physiol 160:504–515. https://doi.org/10.1016/j.cbpa.2011.08.011

Vidal J-P, Martin E, Franchistéguy L, et al (2010) A 50-year high-resolution atmospheric reanalysis over France with the Safran system. Int J Climatol 30:1627–1644. https://doi.org/10.1002/joc.2003

Vindenes Y, Engen S, Saether BE (2011) Integral projection models for finite populations in a stochastic environment. Ecology 92:1146–1156. https://doi.org/10.1890/10-0500.1

Warret Rodrigues C, Angin B, Besnard A (2021) Favoring recruitment as a conservation strategy to improve the resilience of long-lived reptile populations: Insights from a population viability analysis. Ecol Evol 11:13068–13080. https://doi.org/10.1002/ece3.8021

Williams SE, Shoo LP, Isaac JL, et al (2008) Towards an integrated framework for assessing the vulnerability of species to climate change. PLOS Biol 6:e325. https://doi.org/10.1371/journal.pbio.0060325

Winter M, Fiedler W, Hochachka WM, et al (2016) Patterns and biases in climate change research on amphibians and reptiles: a systematic review. R Soc Open Sci 3:160158. https://doi.org/10.1098/rsos.160158

Figure legends

Figure 1. Relationship between mean daily maximum temperatures during gestation (red) and during the mating season (green) and the gestation length, calculated as the difference between the parturition date and 10 June, for female meadow vipers at Mont Ventoux, France. Regression lines and confidence bands from the best model in Table B1 are plotted. Note that a cold summer (lowest values of the red data points) is associated with bimodal parturition dates due to reproductive failure (abortions) in several gravid females.

Figure 2. Relationship between mean daily maximum temperatures during gestation and post-partum body condition (residual of a regression between body mass and body size, A) or clutch success (proportion of live newborns in a clutch, B) for female meadow vipers at Mont Ventoux, France. Regression lines and confidence bands from the best models in Tables B3 and B4 are plotted in panels A and B, respectively. In panel B, the size of the data points is proportional to the total clutch size, which ranges from 2 to 8.

Figure 3. Population viability analysis using an integration projection model (IPM) of the female component of the Mont Ventoux population. A. Elasticity surfaces representing the relative sensitivities of the deterministic growth rate to changes in the kernel function. B. Population viability analysis using a diffusion approximation and simulations of the IBM starting with 100 females randomly drawn from the equilibrium population structure of the deterministic model in the mean environment. Data shown are cumulative quasi-extinction risk during the first 50 years of the simulation for 50,000 population trajectories and three quasi-extinction thresholds (N=1, equivalent to true extinction, N=4 and N=10).

Figure 1

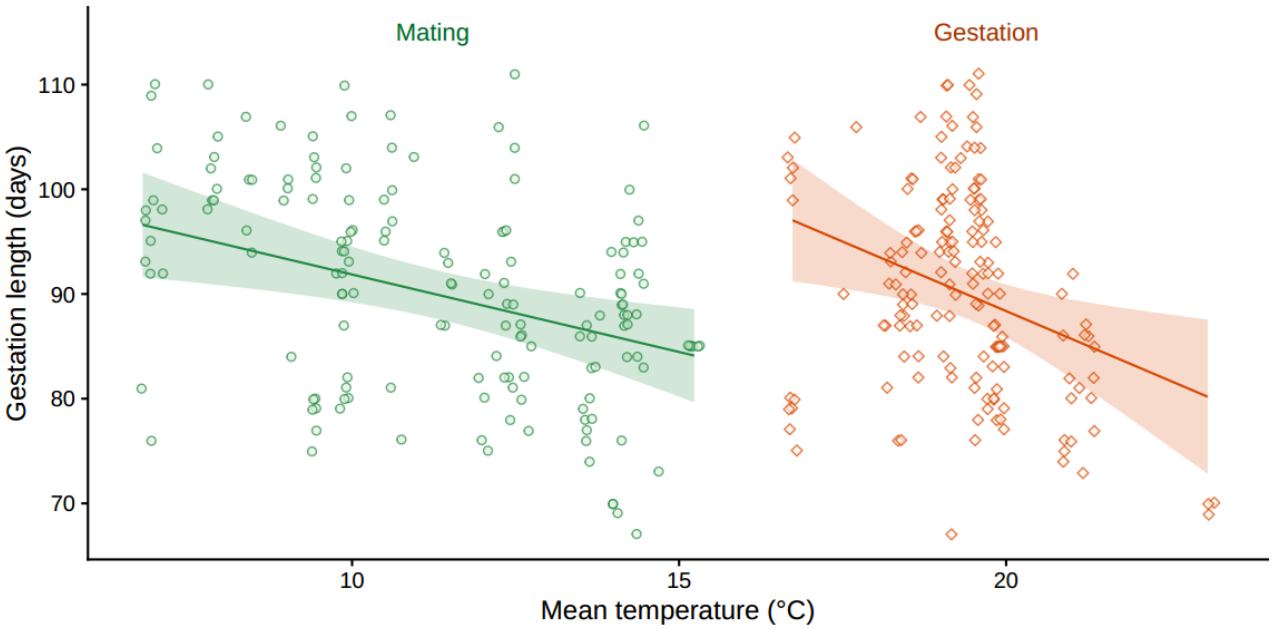
Mating
Gestation
Gestation length (days)
110
100
90
80
70
10
15
20
Mean temperature (°C)

567 **Figure 2**

568

569

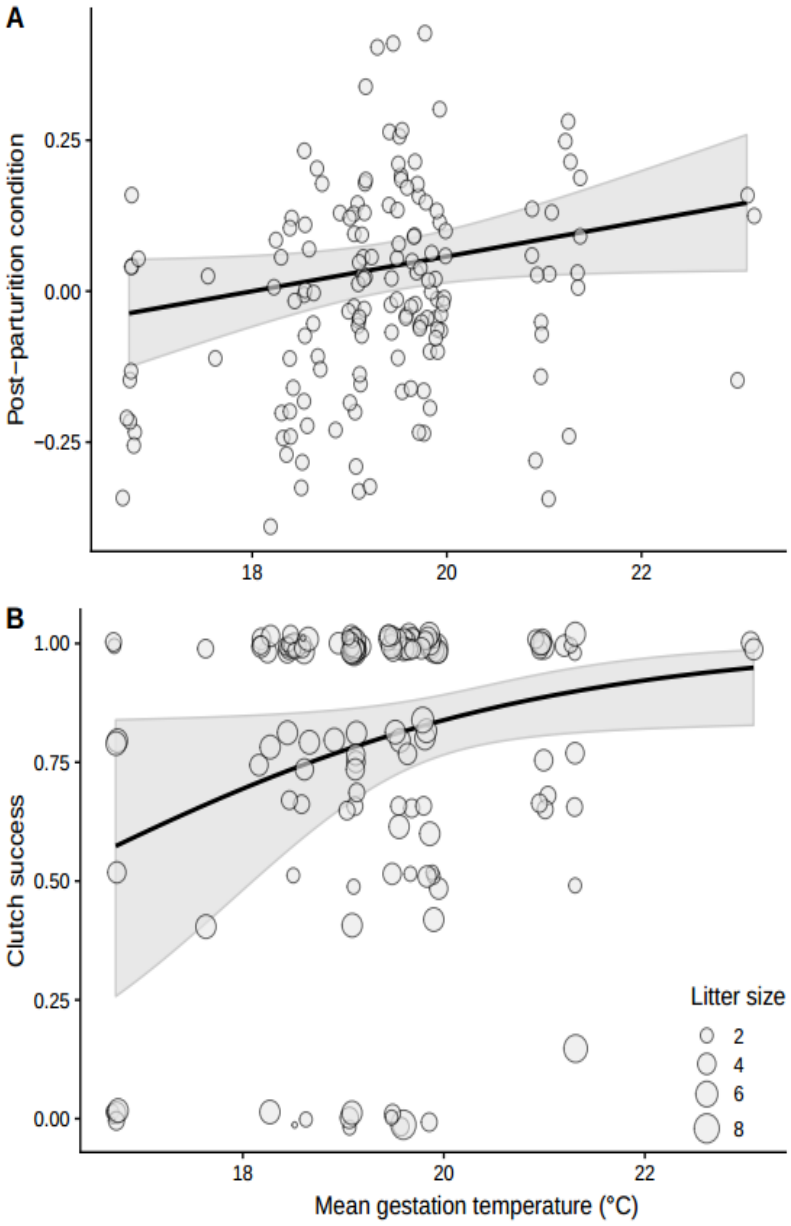

570

Figure 3

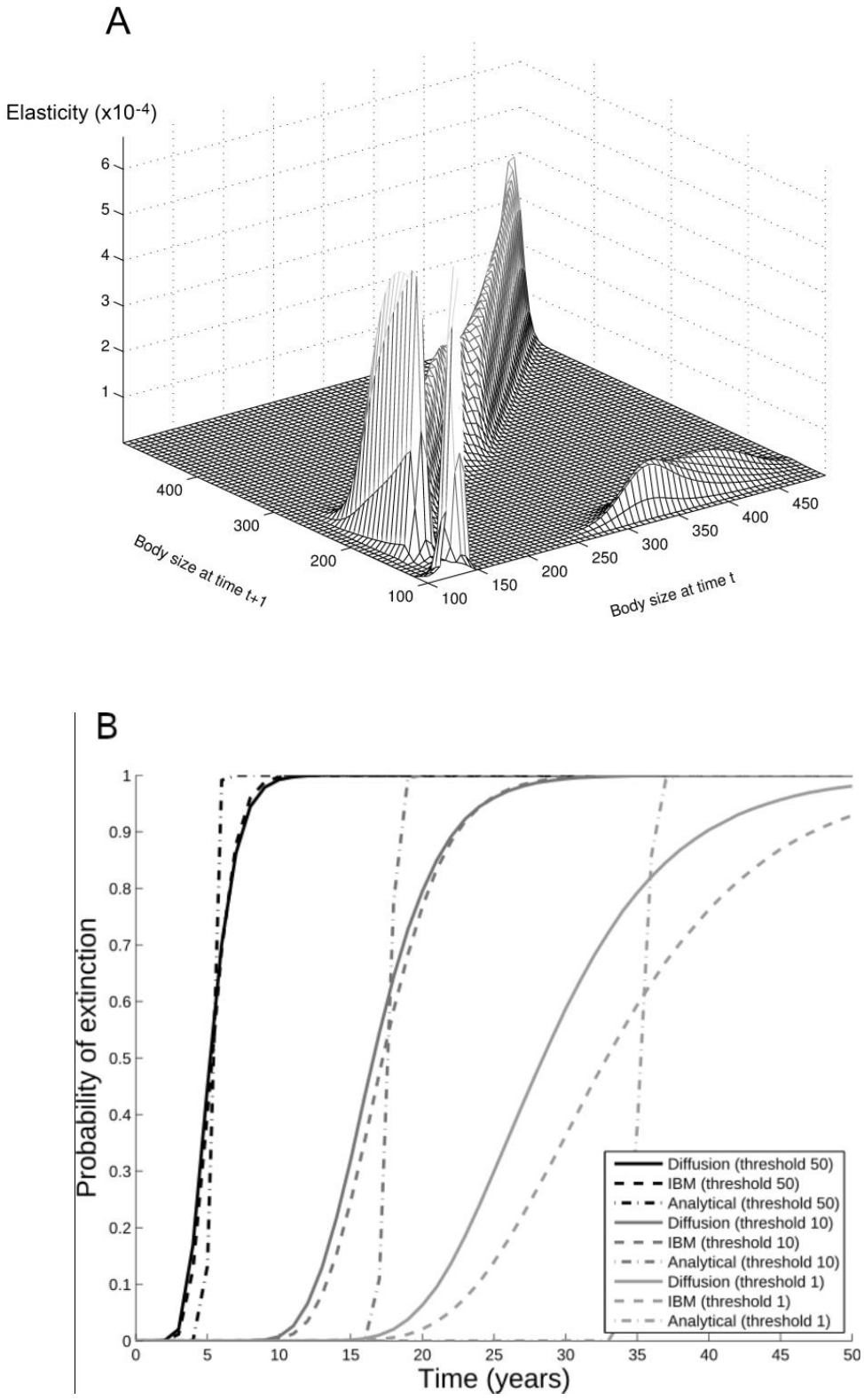
A
Elasticity (x10-4)
6
5
4
3
2
1
400
300
200
100
Body size at time t+1
100
150
200
250
300
350
400
450
Body size at time t
B
Probability of extinction
1
0.9
0.8
0.7
0.6
0.5
0.4
0.3
0.2
0.1
0
0
5
10
15
20
25
30
35
40
45
50
Time (years)
Diffusion (threshold 50)
IBM (threshold 50)
Analytical (threshold 50)
Diffusion (threshold 10)
IBM (threshold 10)
Analytical (threshold 10)
Diffusion (threshold 1)
IBM (threshold 1)
Analytical (threshold 1)

Tables

Table 1. Temporal variation in demographic parameters within the study population of the meadow viper at Mont Ventoux, France. Results shown are number of years (*N*), sample size (*n*), mean (± standard deviation for normal distribution and with 95% CI otherwise), best statistical model from a full model including effects of body size, zone and a random year effects, and the relative temporal variation (RTV). RTV measures the proportion of inter-individual variation caused by yearly variation, and was obtained from variance components of the best model.

Demographic parameter	*N*	*n*	Mean	Best model	RTV
Reproductive traits					
Gestation length*	28	159	90.4 ± 9.81	Year: $\chi^2 = 44.73$, P < 0.001	0.51
Total clutch size	33	220	4.81 ± 1.31	SVL: $F_{1,186} = 58.2$, P < 0.0001 Year: $\chi^2 = 0.001$, P = 0.97	0.001
Clutch success (%)	27	155	0.79 [0.76, 0.82]	SVL: z = -2.01, P = 0.045 Year: $\chi^2 = 107.2$, df = 26, P < 0.0001	0.25
Relative clutch mass (g)	24	152	15.4 ± 5.46	Year: $\chi^2 = 5.23$, P = 0.02	0.12
Post-parturition condition (g)	27	157	30.4 ± 9.02	Zone: $F_{1,128} = 14.99$, P < 0.0001 Year: $\chi^2 = 12.31$, P < 0.0001	0.27
Offspring traits					
Offspring mass (g)	26	494	2.89 ± 0.45	Mother SVL: $F_{1,114} = 4.69$, P = 0.03 Year: $\chi^2 = 188.2$, P < 0.0001	0.11
Offspring condition (residual mass)	26	468	Not applicable (0)	Zone: $F_{1,109} = 3.98$, P = 0.05 Year: $\chi^2 = 18.4$, P < 0.0001	0.21
Annual change in body mass and body size					
Body mass change (g)	20	54	12.6 ± 7.29	Zone: $F_{1,32} = 30.2$, P < 0.0001 Year: $\chi^2 = 13.8$, P = 0.0002	0.59
Body size growth (mm)	22	57	14.6 ± 11.51	Zone: $F_{1,33} = 10.6$, P = 0.003 Year: $\chi^2 = 6.76$, P = 0.009	0.36

* Number of days since June 10 (average ovulation and fertilization date)

SVL = snout to vent length

Supplementary Information

Appendix A – Climate variability

Temperature data calculated for the three reproductive stages of the meadow vipers at the weather station of the study site were strongly and linearly correlated with temperature data collected at the weather station of Carpentras (Pearson's product moment correlation, n = 21 years, mating stage: r = 0.95, P < 0.001; gestation stage: r = 0.93, P < 0.001; non-reproductive stage: r = 0.91, P < 0.001) and with temperature data calculated with the Safran model for the study site (mating stage: r = 0.97, P < 0.001; gestation stage: r = 0.95, P < 0.001; non-reproductive stage: r = 0.94, P < 0.001). To calculate the local weather conditions on the long-term, we thus applied a linear correction factor to the temperature data calculated on the long-term with the Safran model, which was more strongly correlated with local data than data from the Carpentras weather station (mating stage: $F_{1,19}$ = 274.4, P < 0.0001, R^2 = 0.93; gestation stage: $F_{1,20}$ = 176.8, P < 0.0001, R^2 = 0.90; non-reproductive stage: $F_{1,20}$ = 149.7, P < 0.0001, R^2 = 0.88). We obtained similar results when we decomposed data calculated for the gestation into three stages (early gestation, mid-gestation, and late gestation: Pearson's product moment correlations, all r > 0.91; linear regressions, all R^2 > 0.88). Cumulative rainfall data collected at the study site’s weather station were also positively correlated with those from Carpentras’s weather (Pearson's product moment correlation, n = 21 years, mating stage: r = 0.77, P < 0.001; gestation stage: r = 0.88, P < 0.001; non-reproductive stage: r = 0.77, P < 0.001) and those calculated with the Safran model (mating stages: r = 0.93, P < 0.001; gestation stages: r = 0.94, P < 0.001; non-reproductive stage: r = 0.94, P < 0.001). We used a linear correction factor to calculate local rainfall data from data calculated with the Safran model, which correlated more strongly with local data than data from the Carpentras weather station (linear regression, mating stage: $F_{1,20}$ = 126.2, P <

620 0.0001, R^2 = 0.86; gestation stage: $F_{1,21}$ = 152.2, P < 0.0001, R^2 = 0.88; non-reproductive
621 stage: $F_{1,21}$ = 157.7, P < 0.0001, R^2 = 0.89).

622 Temperature, rainfall, global radiation, and humidity varied markedly among years
623 during the long-term study (Figure A1). Late spring and early summer mean temperatures
624 increased weakly throughout the study period (mating stages: + 0.07 °C ± 0.04 s.e. per year,
625 $F_{1,33}$ = 3.16, P = 0.08; early gestation: + 0.08 °C ± 0.03 s.e. per year, $F_{1,33}$ = 6.41, P = 0.02),
626 but this trend wasn't consistent across life stages (other life stages: all P > 0.25, see Figure
627 A1). The rainfall and humidity data showed no consistent temporal trend; instead, they varied
628 in a seemingly random way among years. Global radiation (mean of the cumulative daily
629 global radiation) calculated with the Safran model for the study site increased through time
630 during the study (mating stages: + 15.13 J/cm^2 ± 4.6 s.e. per year, $F_{1,33}$ = 10.55, P = 0.003;
631 gestation: + 7.6 ± 1.7 s.e. per year, $F_{1,33}$ = 20.23, P < 0.0001, Figure A1).

632 Correlations of temperature and rainfall data between reproductive stages within a year
633 were usually small and not significant, but there was a negative correlation between these two
634 environmental factors at the mating and gestation stage, indicating that colder spring and
635 summer climates were also characterized by stronger rainfall (Table A1). Global radiation was
636 consistently positively correlated with temperature and negatively with rainfall within the
637 reproductive stage, and there was also a steady positive correlation between global radiation
638 data across stages within the same year. Humidity was consistently positively correlated with
639 rainfall and temperature within a reproductive stage.

640

Figure A1. We calculated climate conditions for each reproductive year at two life stages of the meadow viper (mating periods [black dots], summer gestation periods [white dots]) from 1980 to 2014. Data from the non-reproductive stage aren't displayed because they had similar temporal trends than data from the gestation stage. (A) Yearly changes in means of maximum daily temperatures (°C); note the exceptionally warm 2003 summer and the warming trend during the mating period represented by the linear regression. (B) Yearly changes in cumulative rainfall (mm); note the wide temporal fluctuations in rainfall during gestation. (C) Yearly changes in daily global radiation (J/cm^2) with the increasing trend over time. (D) Yearly changes in mean daily humidity (g/kg).

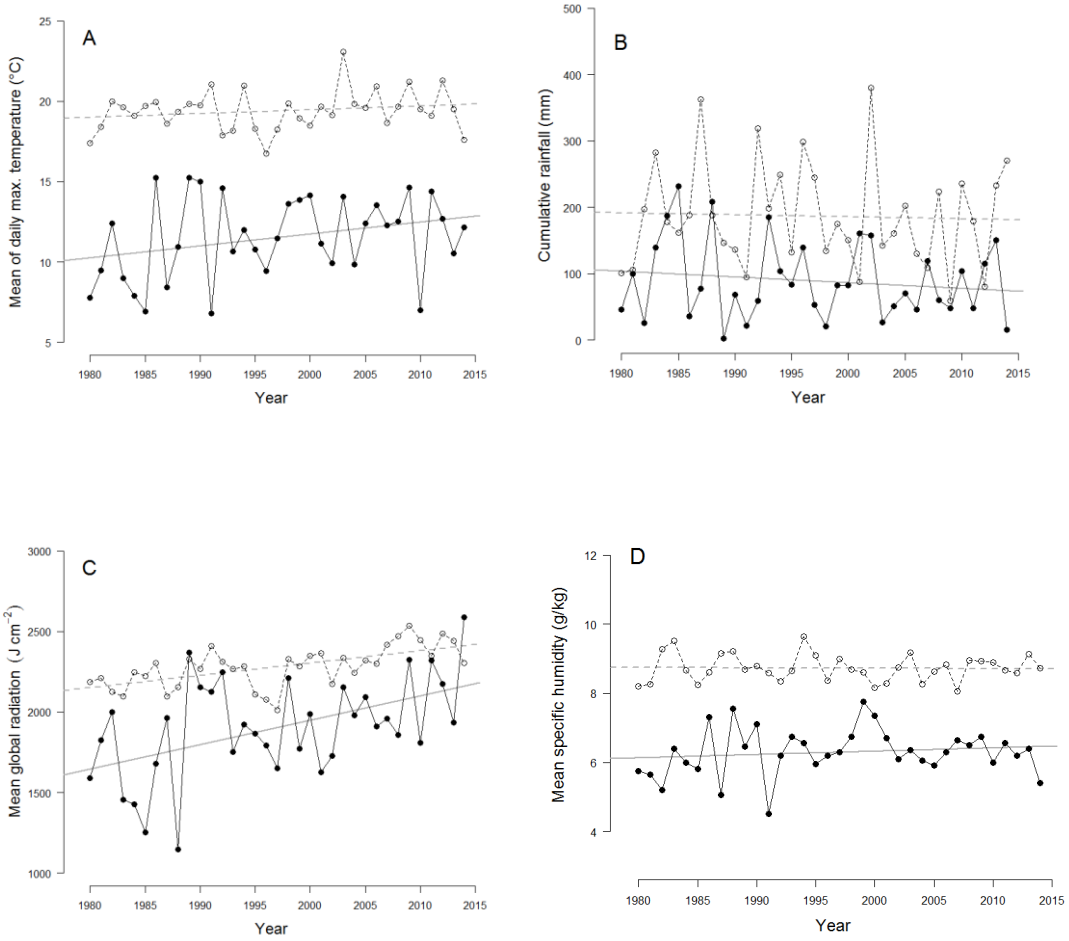

Table A1. Pairwise correlations of temperature (TP), rainfall (RF), global radiation (GR) and specific humidity (SH) data between reproductive stages calculated each year (upper triangular matrix: Pearson's product moment correlation coefficient, lower triangular matrix: sample size). Reproductive stage: M = mating, G = gestation, and NR = non-reproductive stage of the previous year. Bolded correlations are significant without correction for multiple testing ($p < 0.05$).

	TP_M	TP_G	TP_NR	RF_M	RF_G	RF_NR	GR_M	GR_G	GR_NR	SH_M	SH_G	SH_NR
TP_M		0.245	-0.055	**-0.490**	-0.183	-0.051	**0.546**	0.315	0.170	**0.584**	0.039	-0.223
TP_G	*34*		0.056	-0.195	**-0.384**	-0.019	0.181	**0.468**	0.087	0.04	**0.379**	-0.141
TP_NR	*34*	*35*		-0.048	-0.011	-0.212	0.104	0.290	**0.371**	-0.012	-0.139	**0.419**
RF_M	*34*	*34*	*34*		0.163	0.206	**-0.731**	-0.168	-0.114	0.192	-0.048	0.112
RF_G	*34*	*35*	*35*	*34*		0.006	-0.099	**-0.446**	-0.012	-0.153	**0.340**	-0.073
RF_NR	*34*	*35*	*35*	*34*	*35*		-0.185	-0.274	-0.235	0.134	0.321	**0.349**
GR_M	*34*	*34*	*34*	*34*	*34*	*34*		**0.461**	**0.403**	-0.183	-0.037	-0.053
GR_G	*34*	*35*	*35*	*34*	*35*	*35*	*34*		**0.664**	0.173	-0.199	-0.176
GR_NR	*34*	*35*	*35*	*34*	*35*	*35*	*34*	*35*		0.038	-0.135	-0.262
SH_M	*34*	*34*	*34*	*34*	*34*	*34*	*34*	*34*	*34*		-0.023	-0.057
SH_G	*34*	*35*	*35*	*34*	*35*	*35*	*34*	*35*	*35*	*35*		0.141
SH_NR	*34*	*35*	*35*	*34*	*35*	*35*	*34*	*35*	*35*	*35*	*35*	

Appendix B – Model selection tables

Notations in Appendix B are *k* (number of model parameters), LogLikelihood (natural logarithm of the likelihood function), AICc (Akaike Information Criterion corrected for small sample size), Δ_i (difference between the AIC value of the best model and the AIC value for each other models), w_i (Akaike weight), ER (evidence ratio), R^2m (marginal pseudo-R2 for the mixed-effects model) and R^2c (conditional pseudo-R2 for the mixed-effects model). Abbreviations for the descriptions of the covariate are the same as in Table A1. First part corresponds to the kind of climate variable: TP = temperature, GR = global radiation, and SH = specific humidity. Second part corresponds to the kind of life stage: M = mating, G = gestation, and NR = non-reproductive stage of the previous year.

665 **Table B1.** Full set of linear models examining effect of climate variables on gestation length in the meadow viper population at Mont Ventoux,

666 France. The best set of models (models whose cumulative Akaike weight ≤0.95) is in bold. Yellow filling indicates models with $\Delta_i < 2$.

Model rank	Model name	k	-LogLikelihood	AICc	Δ_i	w_i	ER	R^2m	R^2c
1	**TP_M+TP_G**	**5**	**-557.53**	**1125.46**	**0.00**	**0.47**		**0.27**	**0.47**
2	**TP_NR+TP_M+TP_G**	**6**	**-556.58**	**1125.71**	**0.25**	**0.41**	**1.13**	**0.28**	**0.46**
3	**TP_M**	**4**	**-561.17**	**1130.60**	**5.14**	**0.04**	**13.06**	**0.19**	**0.48**
4	**TP_NR+TP_G**	**5**	**-560.28**	**1130.94**	**5.48**	**0.03**	**15.51**	**0.17**	**0.48**
5	TP_G	4	-561.61	1131.49	6.03	0.02	20.34	0.15	0.50
6	TP_NR+TP_M	5	-560.91	1132.21	6.75	0.02	29.15	0.19	0.48
7	GR_M	4	-562.57	1133.40	7.93	0.01	52.81	0.12	0.49
8	1	3	-565.89	1137.94	12.48	0.00	512.75	0.00	0.51
9	TP_NR	4	-565.37	1138.99	13.53	0.00	868.01	0.03	0.51
10	GR_G	4	-565.37	1139.00	13.54	0.00	872.67	0.02	0.51
11	SH_M	4	-565.62	1139.50	14.04	0.00	1117.98	0.01	0.50
12	GR_NR	4	-565.65	1139.56	14.09	0.00	1149.60	0.01	0.51
13	SH_NR	4	-565.80	1139.87	14.41	0.00	1343.79	0.00	0.51
14	SH_G	4	-565.87	1140.00	14.54	0.00	1437.36	0.00	0.51
15	SH_NR+SH_M	5	-565.56	1141.51	16.05	0.00	3055.19	0.01	0.50
16	SH_M+SH_G	5	-565.61	1141.61	16.14	0.00	3203.81	0.01	0.50
17	SH_NR+SH_G	5	-565.79	1141.97	16.51	0.00	3839.25	0.00	0.51
18	SH_NR+SH_M+SH_G	6	-565.55	1143.65	18.19	0.00	8906.16	0.01	0.50

667

668 **Table B2.** Full set of linear models examining effect of climate variables on relative clutch mass in the meadow viper population at Mont

669 Ventoux, France. The best set of models (models whose cumulative Akaike weight ≤ 0.95) is in bold. Yellow filling indicates models with $\Delta_i < 2$.

Model rank	Model name	k	-LogLikelihood	AICc	Δ_i	w_i	ER	R2m	R2c
1	**GR_NR**	**5**	**-453.22**	**916.85**	**0.00**	**0.25**		**0.21**	**0.29**
2	**GR_G**	**5**	**-453.80**	**918.01**	**1.16**	**0.14**	**1.79**	**0.19**	**0.30**
3	**1**	**4**	**-455.13**	**918.54**	**1.69**	**0.11**	**2.33**	**0.17**	**0.29**
4	**SH_G**	**5**	**-454.08**	**918.57**	**1.73**	**0.10**	**2.37**	**0.19**	**0.30**
5	**SH_M+SH_G**	**6**	**-453.84**	**920.26**	**3.41**	**0.05**	**5.50**	**0.19**	**0.30**
6	**TP_M**	**5**	**-454.95**	**920.32**	**3.47**	**0.04**	**5.67**	**0.17**	**0.29**
7	**SH_M**	**5**	**-455.05**	**920.51**	**3.66**	**0.04**	**6.23**	**0.16**	**0.29**
8	**GR_M**	**5**	**-455.05**	**920.51**	**3.67**	**0.04**	**6.26**	**0.17**	**0.29**
9	**SH_NR+SH_G**	**6**	**-453.99**	**920.56**	**3.71**	**0.04**	**6.41**	**0.19**	**0.30**
10	**SH_NR**	**5**	**-455.09**	**920.58**	**3.74**	**0.04**	**6.47**	**0.17**	**0.29**
11	**TP_G**	**5**	**-455.10**	**920.62**	**3.77**	**0.04**	**6.59**	**0.16**	**0.29**
12	**TP_NR**	**5**	**-455.12**	**920.65**	**3.80**	**0.04**	**6.68**	**0.16**	**0.29**
13	**SH_NR+SH_M+SH_G**	**7**	**-453.69**	**922.16**	**5.31**	**0.02**	**14.22**	**0.20**	**0.30**
14	**TP_M+TP_G**	**6**	**-454.86**	**922.30**	**5.45**	**0.02**	**15.29**	**0.16**	**0.29**
15	TP_NR+TP_M	6	-454.95	922.47	5.63	0.01	16.68	0.17	0.29
16	SH_NR+SH_M	6	-454.98	922.54	5.69	0.01	17.22	0.17	0.29
17	TP_NR+TP_G	6	-455.09	922.77	5.92	0.01	19.33	0.16	0.29
18	TP_NR+TP_M+TP_G	7	-454.86	924.50	7.65	0.01	45.90	0.16	0.29

670

671

672 **Table B3.** Full set of linear models examining effect of climate variables on post-parturition condition in the meadow viper population at Mont
673 Ventoux, France. The best set of models (models whose cumulative Akaike weight ≤ 0.95) is in bold. Yellow filling indicates models with $\Delta_i < 2$.

Model rank	Model name	k	-LogLikelihood	AICc	Δ_i	w_i	ER	R2m	R2c
1	**TP_NR+TP_G**	**7**	**92.11**	**-169.45**	**0.00**	**0.18**		**0.81**	**0.84**
2	**TP_NR**	**6**	**90.76**	**-168.94**	**0.51**	**0.14**	**1.29**	**0.80**	**0.84**
3	**TP_NR+TP_M+TP_G**	**8**	**92.73**	**-168.45**	**1.01**	**0.11**	**1.65**	**0.82**	**0.84**
4	**GR_NR**	**6**	**90.42**	**-168.27**	**1.19**	**0.10**	**1.81**	**0.80**	**0.83**
5	**TP_G**	**6**	**90.42**	**-168.25**	**1.20**	**0.10**	**1.82**	**0.81**	**0.84**
6	**TP_M+TP_G**	**7**	**91.43**	**-168.08**	**1.37**	**0.09**	**1.99**	**0.81**	**0.84**
7	**1**	**5**	**88.74**	**-167.06**	**2.39**	**0.05**	**3.30**	**0.79**	**0.84**
8	**TP_NR+TP_M**	**7**	**90.90**	**-167.03**	**2.43**	**0.05**	**3.36**	**0.81**	**0.84**
9	**GR_G**	**6**	**89.61**	**-166.65**	**2.80**	**0.04**	**4.06**	**0.80**	**0.83**
10	**TP_M**	**6**	**89.06**	**-165.53**	**3.92**	**0.03**	**7.09**	**0.80**	**0.84**
11	**SH_M**	**6**	**89.00**	**-165.43**	**4.02**	**0.02**	**7.48**	**0.80**	**0.84**
12	**GR_M**	**6**	**88.88**	**-165.18**	**4.27**	**0.02**	**8.46**	**0.79**	**0.84**
13	SH_NR	6	88.75	-164.91	4.54	0.02	9.67	0.79	0.84
14	SH_G	6	88.74	-164.91	4.54	0.02	9.69	0.79	0.84
15	SH_NR+SH_M	7	89.00	-163.23	6.22	0.01	22.43	0.80	0.84
16	SH_M+SH_G	7	89.00	-163.23	6.22	0.01	22.44	0.80	0.84
17	SH_NR+SH_G	7	88.75	-162.73	6.72	0.01	28.81	0.79	0.84
18	SH_NR+SH_M+SH_G	8	89.00	-161.00	8.45	0.00	68.39	0.80	0.84

674
675

Table B4. Full set of binomial models examining effect of climate variables on clutch success in the meadow viper population at Mont Ventoux, France. The best set of models (models whose cumulative Akaike weight ≤ 0.95) is in bold. Yellow filling indicates models with $\Delta_i < 2$. The set of models did not include GR_M effect due to lack of convergence.

Model rank	Model name	k	-LogLikelihood	AICc	Δ_i	w_i	ER	R2m	R2c
1	**TP_NR+TP_G**	**5**	**-157.85**	**326.10**	**0.00**	**0.21**		**0.06**	**0.10**
2	**TP_G**	**4**	**-159.13**	**326.53**	**0.43**	**0.17**	**1.24**	**0.04**	**0.09**
3	**SH_NR**	**4**	**-159.76**	**327.79**	**1.69**	**0.09**	**2.32**	**0.02**	**0.09**
4	**TP_NR+TP_M+TP_G**	**6**	**-157.85**	**328.27**	**2.16**	**0.07**	**2.95**	**0.06**	**0.10**
5	**TP_M+TP_G**	**5**	**-159.08**	**328.56**	**2.46**	**0.06**	**3.42**	**0.05**	**0.09**
6	**1**	**3**	**-161.27**	**328.70**	**2.60**	**0.06**	**3.66**	**0.00**	**0.07**
7	**SH_NR+SH_M**	**5**	**-159.32**	**329.04**	**2.94**	**0.05**	**4.35**	**0.03**	**0.09**
8	**SH_M**	**4**	**-160.46**	**329.19**	**3.09**	**0.05**	**4.69**	**0.01**	**0.08**
9	**SH_NR+SH_G**	**5**	**-159.50**	**329.40**	**3.30**	**0.04**	**5.20**	**0.03**	**0.09**
10	**TP_NR**	**4**	**-160.67**	**329.60**	**3.50**	**0.04**	**5.76**	**0.09**	**0.08**
11	**TP_M**	**4**	**-160.97**	**330.21**	**4.11**	**0.03**	**7.81**	**0.10**	**0.08**
12	**GR_NR**	**4**	**-161.03**	**330.33**	**4.23**	**0.03**	**8.27**	**0.01**	**0.08**
13	**SH_G**	**4**	**-161.09**	**330.45**	**4.34**	**0.02**	**8.78**	**0.01**	**0.07**
14	**SH_NR+SH_M+SH_G**	**6**	**-158.94**	**330.45**	**4.35**	**0.02**	**8.78**	**0.04**	**0.09**
15	GR_G	4	-161.12	330.50	4.40	0.02	9.02	0.01	0.07
16	SH_M+SH_G	5	-160.14	330.68	4.58	0.02	9.89	0.02	0.07
17	TP_NR+TP_M	5	-160.47	331.35	5.25	0.02	13.82	0.01	0.09

682 **Table B5.** Full set of linear models examining effect of climate variables on offspring mass at birth in the meadow viper population at Mont

683 Ventoux, France. The best set of models (models whose cumulative Akaike weight ≤ 0.95) is in bold. Yellow filling indicates models with $\Delta_i < 2$.

Model rank	Model name	k	-LogLikelihood	AICc	Δ_i	w_i	ER	R2m	R2c
1	**1**	**6**	**-192.89**	**397.95**	**0.00**	**0.15**		**0.05**	**0.61**
2	**GR_NR**	**7**	**-192.30**	**398.84**	**0.88**	**0.09**	**1.55**	**0.06**	**0.61**
3	**TP_NR**	**7**	**-192.33**	**398.89**	**0.94**	**0.09**	**1.60**	**0.06**	**0.61**
4	**TP_G**	**7**	**-192.41**	**399.06**	**1.10**	**0.08**	**1.73**	**0.05**	**0.61**
5	**GR_M**	**7**	**-192.59**	**399.41**	**1.46**	**0.07**	**2.07**	**0.05**	**0.60**
6	**TP_NR+TP_G**	**8**	**-191.59**	**399.48**	**1.52**	**0.07**	**2.14**	**0.07**	**0.61**
7	**TP_M**	**7**	**-192.68**	**399.58**	**1.63**	**0.07**	**2.25**	**0.05**	**0.60**
8	**GR_G**	**7**	**-192.83**	**399.89**	**1.94**	**0.06**	**2.64**	**0.05**	**0.61**
9	**SH_M**	**7**	**-192.87**	**399.97**	**2.02**	**0.05**	**2.74**	**0.05**	**0.61**
10	**SH_NR**	**7**	**-192.88**	**399.99**	**2.03**	**0.05**	**2.76**	**0.05**	**0.61**
11	**SH_G**	**7**	**-192.89**	**400.01**	**2.06**	**0.05**	**2.80**	**0.05**	**0.61**
12	**TP_NR+TP_M**	**8**	**-192.17**	**400.64**	**2.69**	**0.04**	**3.83**	**0.06**	**0.61**
13	**TP_M+TP_G**	**8**	**-192.31**	**400.91**	**2.95**	**0.03**	**4.38**	**0.05**	**0.60**
14	**TP_NR+TP_M+TP_G**	**9**	**-191.55**	**401.47**	**3.51**	**0.03**	**5.79**	**0.07**	**0.61**
15	SH_NR+SH_M	8	-192.86	402.01	4.05	0.02	7.58	0.05	0.61
16	SH_M+SH_G	8	-192.87	402.04	4.08	0.02	7.69	0.05	0.61
17	SH_NR+SH_G	8	-192.88	402.05	4.10	0.02	7.76	0.05	0.61
18	SH_NR+SH_M+SH_G	9	-192.85	404.08	6.12	0.01	21.37	0.05	0.61

684

685

686 **Table B6.** Full set of linear models examining effect of climate variables on offspring body condition at birth in the meadow viper population at

687 Mont Ventoux, France. The best set of models (models whose cumulative Akaike weight ≤ 0.95) is in bold.

Model rank	Model name	k	-LogLikelihood	AICc	Δ_i	w_i	ER	R2m	R2c
1	**GR_G**	**8**	**10.24**	**-4.17**	**0.00**	**0.54**		**0.63**	**0.80**
2	**TP_G**	**8**	**8.72**	**-1.13**	**3.04**	**0.12**	**4.58**	**0.63**	**0.80**
3	**GR_NR**	**8**	**8.18**	**-0.04**	**4.13**	**0.07**	**7.87**	**0.61**	**0.80**
4	**TP_M+TP_G**	**9**	**8.92**	**0.56**	**4.73**	**0.05**	**10.63**	**0.63**	**0.80**
5	**TP_NR+TP_G**	**9**	**8.82**	**0.75**	**4.92**	**0.05**	**11.70**	**0.63**	**0.80**
6	**1**	**7**	**6.38**	**1.48**	**5.66**	**0.03**	**16.91**	**0.61**	**0.81**
7	**TP_NR+TP_M+TP_G**	**10**	**9.08**	**2.32**	**6.49**	**0.02**	**25.68**	**0.63**	**0.80**
8	**TP_M**	**8**	**6.94**	**2.43**	**6.60**	**0.02**	**27.17**	**0.62**	**0.81**
9	**GR_M**	**8**	**6.88**	**2.55**	**6.72**	**0.02**	**28.75**	**0.62**	**0.81**
10	**SH_G**	**8**	**6.70**	**2.92**	**7.09**	**0.02**	**34.69**	**0.62**	**0.81**
11	**TP_NR**	**8**	**6.62**	**3.06**	**7.24**	**0.01**	**37.26**	**0.61**	**0.80**
12	SH_M	8	6.41	3.50	7.67	0.01	46.32	0.61	0.81
13	SH_NR	8	6.38	3.55	7.72	0.01	47.52	0.61	0.81
14	TP_NR+TP_M	9	7.32	3.76	7.93	0.01	52.76	0.61	0.80
15	SH_M+SH_G	9	6.71	4.98	9.15	0.01	96.97	0.62	0.81
16	SH_NR+SH_G	9	6.70	5.00	9.17	0.01	98.07	0.62	0.81
17	SH_NR+SH_M	9	6.41	5.57	9.74	0.00	130.45	0.61	0.81
18	SH_NR+SH_M+SH_G	10	6.71	7.07	11.24	0.00	275.50	0.62	0.81

688

Appendix C – Integral projection model

Model rationale

The integral projection model (IPM) assumes that the life history is structured by body size (here, snout-vent length), hereafter called *y*, such that snakes differ by *y* only and *y* is the sole determinant of their vital rates. The population can then be described by a function $N(y,t)$ where $N(y,t)dy$ is the discrete number of individuals between size values y and $y+dy$ at time t. The total, finite population size is called $N(t)$. To describe this population in a fluctuating environment, we used a stochastic IPM formulated by Vindenes et al. (2011):

$$N(y,t+1) = \int_{\Omega} K(y,x,Z_t)N(x,t)dx, \qquad \text{(C1)}$$

$$K(y,x,Z_t) = s(x,Z_t)\,f_s(y,x,Z_t) + b(x,Z_t)\,f_b(y,x,Z_t)$$

where K is a stochastic projection kernel, Z_t is a random vector describing parameter values at time *t* and thus the environmental state, and Ω is the domain of possible values for body size (Rees and Ellner 2009).

The kernel describes transition rates from state *x* at time *t* to state *y* at time *t+1* in environment *Z*. According to equation (C1), the kernel is decomposed into (1) the survival-growth kernel where $s(x,Z_t)$ is the survival probability of an individual with trait value *x*, and $f_s(y,x,Z_t)dy$ is the probability of reaching trait value between y and $y+dy$ at time *t+1* for an individual of trait value *x*, and (2) the fecundity kernel where $b(x,Z_t)$ is the fecundity of an individual with trait value *x*, and $f_b(y,x,Z_t)$ is the probability density function of the trait value of offspring. Thus, the stochastic model described by equation (C1) is similar the deterministic model of Easterling *et al.* (2000) conditional on *Z*.

This IPM can be considered as a stochastic matrix projection model (MPM) with an infinite number of discrete classes. According to the seminal paper by Easterling *et al.* (2000), most of the properties of MPMs can therefore be generalised to IPMs, including the calculation of the deterministic population growth rate λ, equilibrium population structure, reproductive values and deterministic elasticities of λ. Here, we used a numerical method to simulate the deterministic IPMs by discretising the state-space Ω into *C* classes of the same width Δy and computing integrals using Simpson's 3/8 method, a more accurate numerical integration method than the standard mid-point rule (Merow et al. 2014).

For stochastic environments and finite populations, we used individual based simulations and considered that Z_t is a vector of year-specific parameters and assumed that parameter values vary randomly over time according to the random effects model of Rees and Ellner (2009). This implies that elements of the stochastic kernel of the IPM are drawn randomly each year from some parametric statistical distributions. The dynamics of the expected population size at time *t+1* given population size at time *t* can then be written as:

$$E\left[N(t+1)\middle|N(t)\right] = \int_{\Omega}\int_{\Omega} \bar{k}(y,x)N(x,t)dxdy \qquad \text{(C2)}$$

where $\bar{k}(y,x)$ is the mean kernel defined by averaging the stochastic kernel over all possible environmental state values. This dynamics is characterised by an expected growth rate $\overline{\lambda}$ and a stable size structure $\bar{u}(x)$.

An important property of this stochastic IPM is the long-run logarithmic growth rate, denoted $\ln \lambda_s$, which describes the asymptotic exponential growth rate of the population size after a sufficiently long time (Lande et al. 2003; Rees and Ellner 2009; Tuljapurkar 1990). The long-run logarithmic growth rate can be approximated assuming a small environmental noise, which implies

that the population stays close to its stable distribution (e.g., for IPM Rees and Ellner 2009). Vindenes et al. (2011) showed that the first-order approximation of the long-run growth rate of the stochastic IPM writes like:

$$\ln \lambda_s \approx \ln \bar{\lambda} - \frac{\sigma_e^2}{2\bar{\lambda}^2} - \frac{\sigma_d^2}{2\bar{\lambda}^2 V}, \qquad \text{(C3)}$$

where $\bar{\lambda}$ is the deterministic population growth rate of the mean kernel, σ_e^2 is the environmental variance (i.e., a consequence of between-year deviation from the mean kernel of the average individual contribution to total reproductive value), σ_d^2 is the demographic variance (i.e., a consequence within-year deviation from the mean of the year of the individual contribution to total reproductive value) and V is the total reproductive value (i.e., equivalent to population size when the population reaches the stable distribution). We calculated σ_e^2 by numeric simulations of the growth rate, estimated σ_d^2 from the slope of the regression of the mean exponential growth rate against the inverse population size, and then simulated model (C2) with a diffusion approximation of long-run growth rate following the numerical methods of Vindenes et al. (2011).

Model parameterization

Our female life cycle for the meadow viper counts individuals from the age of one year and assumes annual reproduction followed by annual survival and body growth of juveniles, and the annual survival, body growth and sexual maturation of immature individuals (until six years old, equivalent to 7 age classes of immature individuals). Juvenile survival increases with offspring mass at birth, which itself depends on offspring body size (snout-vent length, mm) that is influenced by maternal body size and total clutch size. Maturation probability depends on both body size and age of the female, and occurs around 4 to 6 years old. Once maturity is reached, females alternate regularly breeding and non-breeding years (equivalent to two breeding classes of mature

individuals) and their fecundity increases with body size. To calculate the number of viable offspring produced by breeding females each year, we estimated fecundity (total clutch size), clutch success (percentage of viable offspring within a clutch) and female sex ratio. This complex life cycle was modelled with an IPM including both a continuous size structure and nine discrete categories. The first seven discrete categories were age classes (from 0 to 6 years) for immature individuals, and the two last discrete categories included the breeding and non-breeding states for mature individuals. There is significant environmental variation for annual juvenile survival, body size at birth and reproduction through clutch success. This life history is based on earlier results (Baron et al., 2010a, Baron et al., 2013, Baron et al., 2010b) and results from the current study.

The IPM for this complex life cycle can be written like:

$$n(y,t+1) = \int_Y k(y,x) \times n(x,t) \times dx, \qquad \text{(C4)}$$

where $n(y,t)$ is a vector of functions describing the size distribution in each class, and k is a matrix of functions whose elements are kernel elements of a classical IPM for each transition between classes. More precisely, we can write down the matrix k like:

$$k(y,x) = \begin{pmatrix} 0 & 0 & 0 & 0 & 0 & 0 & 0 & k_F & 0 \\ k_{0\to1} & 0 & 0 & 0 & 0 & 0 & 0 & 0 & 0 \\ 0 & k_{1\to2} & 0 & 0 & 0 & 0 & 0 & 0 & 0 \\ 0 & 0 & k_{2\to3} & 0 & 0 & 0 & 0 & 0 & 0 \\ 0 & 0 & 0 & k_{3\to4} & 0 & 0 & 0 & 0 & 0 \\ 0 & 0 & 0 & 0 & k_{4\to5} & 0 & 0 & 0 & 0 \\ 0 & 0 & 0 & 0 & 0 & k_{5\to6} & 0 & 0 & 0 \\ k_{0\to B} & k_{1\to B} & k_{2\to B} & k_{3\to B} & k_{4\to B} & k_{5\to B} & k_{6\to B} & k_{B\to B} & k_{NB\to B} \\ 0 & 0 & 0 & 0 & 0 & 0 & 0 & k_{B\to NB} & k_{NB\to NB} \end{pmatrix} \qquad \text{(C5)}$$

where elements of this matrix are listed below:

$$k_{i\to j}(y,x) = \left(1 - \Pi_m(y,i+1)\right) \times f_{Im}(y,x) \times \phi_{Im}$$

771 $$k_F(y,x) = \left[\sum_{k=1}^{F_{max}} \Pi(F_0(x) = k) \times k \times f_F(y, x \mid F_0(x) = k) \right] \times p_{cs}(x) \times p_f \times \phi_0(m(y))$$

772 $$k_{i \to B}(y,x) = \Pi_m(y, i+1) \times f_i(y,x) \times \phi_{Im}$$

773 $$k_{B \to B}(y,x) = P_{B \to B} \times f_B(y,x) \times \phi_A$$

774 $$k_{NB \to B}(y,x) = P_{NB \to B} \times f_{NB}(y,x) \times \phi_A$$

775 $$k_{B \to NB}(y,x) = P_{B \to NB} \times f_B(y,x) \times \phi_A$$

776 $$k_{NB \to NB}(y,x) = P_{NB \to NB} \times f_{NB}(y,x) \times \phi_A$$

777

778 Parameters values for the different terms of these elements are provided in Table C1 averaging
779 across the two study sites. The stochastic model included inter-annual variation in clutch success, size
780 at birth and size growth of non-reproductive females (this study) as well as early juvenile survival
781 (Baron et al., 2010a, Baron et al., 2013, Baron et al., 2010b). The stochastic version was analysed
782 with an individual based model in Python whereas the deterministic version was fitted with Matlab.
783 Default parameter values of the deterministic model provided a good fit to the average size
784 distribution in the study population (see Figure C1)

785

786

787 **Figure C1.** Comparison between the size distribution predicted by the IPM and the observed size
788 distribution in the pooled sample of females corrected for unequal capture probabilities. The two
789 statistical distributions looked similar although the IPM tended to predict more of the small juvenile
790 size classes and less of the old adults' size classes than observed (χ^2 test, $P < 0.0001$).
791

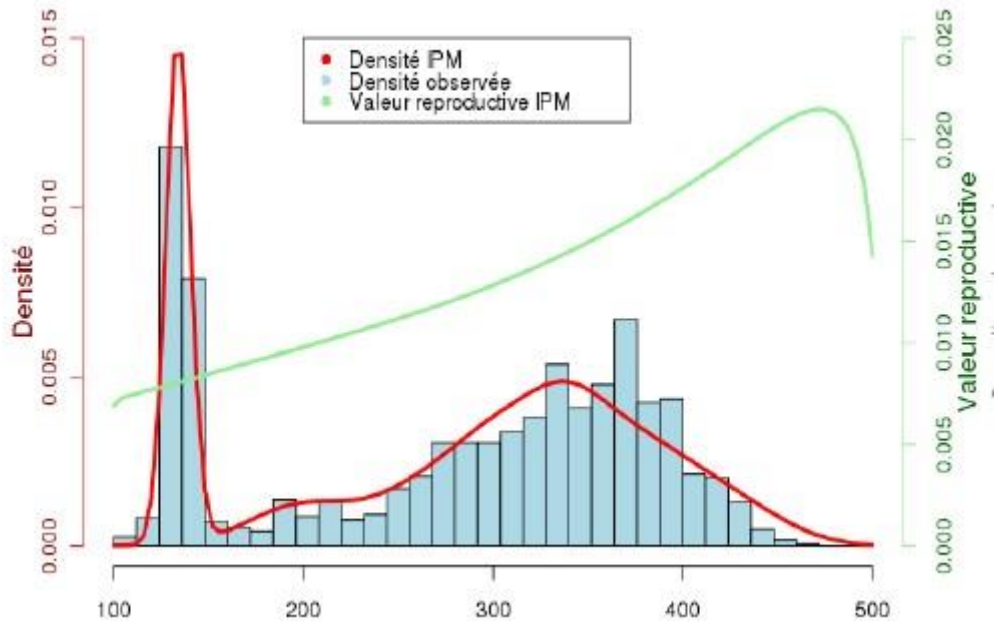

792
793
794

795 **Table C1:** Model parameters when size is estimated by snout-vent length (SVL, mm) for *Vipera ursinii*
796 *ursinii* at Mont Ventoux, France. The table provides the mean and error of the mean in the scale of the
797 statistical model used to estimate parameters, as well as inter-annual SD, statistical procedure / software and
798 kinds of distribution (glm: generalized linear model, lm: linear model, glmmPQL: generalized linear mixed
799 model with penalized quasi-likeihood, vglm: vector generalized linear model, lme: liner mixed model,
800 MARK CJS: Cormak-Jolly-Seber open population model including multi-state models).

Trait	***Scale***	***Estimate***	***SE***	***Inter-annual SD***	***Procedure***	***Distribution***
Sexual maturation probability - $\Pi_m(y,i)$						
Intercept	Logit	-24.030	5.88	0	glm	Binomial
Slope age i	Logit	2.072	0.530	0		
Slope SVL y	Logit	0.050	0.017	0		
Size of immature females at time $t+1$ - $f_{Im}(y,x)$						
Intercept	Identity	83.646	10.82	0	lm	Gaussian
Slope SVL x	Identity	0.8267	0.043	0		
Residual variance*	Power	321097	NA			
Annual survival of immature females - ϕ_{Im}						
Mean value	Logit	1.202	0.467	0	MARK CJS	Binomial
Fecundity (total clutch size) - $F_0(x)$						
λ - Mean value	elogit	-1.665	0.294	0	vglm	Generalised
Θ - Intercept	log	-1.090	0.285	0		Poisson
Θ - Slope SVL x	log	0.007	0.0007	0		
Clutch success - $p_{cs}(x)$						
Intercept	Logit	3.662	1.822	1.139	glmmPQL	Binomial
Slope maternal SVL x	Logit	-0.024	0.323	0		
Residual variance	Logit	1.067	NA			
Size at birth given fecundity - $f_F(y,x \mid F_0(x))$						
Intercept	Identity	116.895	4.14	4.064	lme	Gaussian
Slope maternal SVL x	Identity	0.0608	0.012	0		
Slope fecundity $F_0(x)$	Identity	-1.389	0.351	0		
Residual variance	Identity	6.143	NA			
Female sex ratio - p_f						
Intercept	Logit	-0.044	0.1054		glm	Binomial

Juvenile survival as a function of standardised body mass at birth - $\phi_0(m(y))$						
Intercept	Logit	-0.442	0.505	0.269	MARK CJS	Binomial
Slope body mass *m(y)*	Logit	0.837	0.539	0		
Relationship between mass at birth and size at birth - $m(y)$						
Intercept	Identity	-3.393	0.276	0	lm	Gaussian
Slope size at birth *y*	Identity	0.047	0.002	0		
Residual variance	Identity	0.2933	NA			
Transition from breeding to non-breeding state - $P_{B\to NB}$						
Mean value	Logit	3.200	0.524	0	MARK CJS	Binomial
Size of breeding females at time $t+1$ - $f_B(y,x)$						
Intercept	Identity	21.559	14.76	0	lm	Gaussian
Slope SVL *x*	Identity	0.9514	0.039	0		
Residual variance	Identity	9.04	NA			
Adult survival - ϕ_A						
Mean value	Logit	0.789	0.116	0	MARK CJS	Binomial
Transition from non-breeding to breeding state - $P_{NB\to B}$						
Mean value	Logit	1.756	0.391	0	MARK CJS	Binomial
Size of non-breeding females at time $t+1$ - $f_{NB}(y,x)$						
Intercept	Identity	84.821	21.88	1.23	lm	Gaussian
Slope SVL *x*	Identity	0.8204	0.058	0		
Residual variance	Identity	11.43	NA			

801 * Residual variance is modelled like a power function of predicted values (power exponent: -1.79)

802